

Supporting Information for

Striking Increase of Hole Mobility Upon Metal Coordination to Tri-phenylene-Schiff-Base Semiconducting Multicolumnar Mesophases.

*Estela de Domingo,^a César L. Folcia,^b Josu Ortega,^c Jesús Etxebarria,^b Roberto Termine,^d Attilio Golemme,^d Silverio Coco,^{*a} and Pablo Espinet.^{*a}*

^a IU CINQUIMA/Química Inorgánica, Facultad de Ciencias, Universidad de Valladolid, 47071 Valladolid, Castilla y León, Spain. ^b Condensed Matter Physics, University of the Basque Country, UPV/EHU, 48080 Bilbao, Spain. ^c Applied Physics II, University of the Basque Country, UPV/EHU, 48080 Bilbao, Spain. ^d LASCAMM CR-INSTM, CNR-Nanotec, Dipartimento di Fisica, Università della Calabria, 87036 Rende, Italy..

** e-mail addresses: silverio.coco@uva.es; espinet@qi.uva.es*

Table of Contents

Experimental section	Page S2
UV-Visible data	Page S13
¹H NMR spectra	Page S14
¹³C{¹H} NMR spectra	Page S19
MALDI-TOF mass spectra	Page S24
DSC scans	Page S30
Electrochemical Studies	Page S36
Charge Mobility measurements	Page S37
Low-angle X-ray diffraction diagrams	Page S39
References	Page S42

EXPERIMENTAL SECTION

General Considerations. General procedures are as reported before. Elemental analyses were performed by the “Servicio de análisis elemental, CACTI, Universidad de Vigo”. IR spectra were recorded on a Perkin-Elmer Frontier spectrometer coupled to a Pike GladiATR-210 accessory. NMR spectra were recorded on Bruker AV-400 or Varian 500 instruments in CDCl₃. MALDI-TOF MS was performed using a Bruker Daltonics autoflex speed instrument equipped with nitrogen laser (340 nm). Positive-ion mode spectra were recorded using the reflective mode. The accelerating voltage was 19 kV. The analytical sample was obtained by mixing the dichloromethane solution of the sample (1 mg/mL) and dichloromethane solution of the matrix (DCTB, 10 mg/mL) in a 1/5 (vol/vol) ratio. The prepared solution of the sample and the matrix (0.5 μ L) was loaded on the MALDI plate and allowed to dry at 23°C before the plate was inserted into the vacuum chamber of the MALDI instrument. UV/Vis absorption spectra were obtained by means of a Shimadzu UV-2550 spectrophotometer, in dichloromethane ($\sim 1 \times 10^{-5}$ M).

Microscopy studies were carried out on a Leica DMRB microscope equipped with a Mettler FP82HT hot stage and a Mettler FP90 central processor, at a heating rate of 10 °C min⁻¹. DSC was performed using a DSC Q20 from TA Instruments with samples (2–5 mg) sealed in aluminum pans and a scanning rate of 10 °C/min under a nitrogen atmosphere.

The diffraction diagrams were recorded using a Stoe Stadivari goniometer equipped with a Genix3D microfocus generator (Xenocs) and a Dectris Pilatus 100K detector. Temperature control was achieved using a nitrogen-gas Cryostream controller (Oxford Cryosystems) allowing for a temperature control of about 0.1 °C. The materials were viscous enough to be held in loops of 300 – 500 μ m of diameter (MiTeGen). The exposure time was 5 minutes. Monochromatic Cu-K α_1 radiation ($\lambda = 1.5418$ Å) was used.

Electrochemical studies employed cyclic voltammetry using a potentiostat EG&G model 273. The three-electrode system was equipped with a platinum (3 mm diameter) working electrode, a saturated calomel reference electrode (SCE), and a Pt wire counter electrode. The electrochemical potentials were calibrated relative to SCE using ferrocene as an internal standard (Fc/Fc^+) at +0.46 V vs. SCE). Tetra-n-butylammonium hexafluorophosphate (0.1 M) in CH_2Cl_2 was used as a supporting electrolyte and the solutions of the complexes were in the order 10^{-3} M. All scans were done at 100 mV s^{-1} .

Literature methods were used for the synthesis of methyl 4-(6-bromohexyloxy)benzoate,¹ monohydroxy-3,6,7,10,11-pentakis(dodecyloxy)triphenylene,² 2,3,6,7,10,11-hexakis(dodecyloxy)triphenylene (**TriPh**),³ and N,N'-ethylenedisalicyldeneamine (Salen) copper,⁴ nickel⁵ and vanadyl complexes.⁶

Only examples are described, as the syntheses were similar for the rest of the complexes. Yields, IR, and analytical data are given for all the complexes.

Preparation of methyl 4-[6-(3,6,7,10,11-pentadodecyloxytriphenylen-2-oxy)hexyloxy]benzoate

To a solution of 2-hydroxy-3,6,7,10,11-pentakis(dodecyloxy)triphenylene (2.72 g, 2.33 mmol) and methyl 4-(6-bromohexyloxy)benzoate (2.57 g, 8.17 mmol) in 80 mL of dry butanone, K_2CO_3 (1.15 g, 8.28 mmol) was added. The mixture was refluxed for 16 h. Butanone was distilled off, dichloromethane (150 mL) was added and the mixture treated with water. The organic phase was dried over magnesium sulfate and evaporated to dryness. Purification by column chromatography (silica gel with hexane/dichloromethane 1/2 as eluent) yielded 2.46 g (75 %) of a white solid. IR (ν , cm^{-1}) 1724 (vs, $\text{C}=\text{O}$). ^1H NMR (500 MHz, CDCl_3): δ 7.97 (d, 2H^A , **ArH**, AA' part of $\text{AA}'\text{XX}'$ spin system ($N_{A,X} = J_{A,X} + J_{A,X'} = 9.0 \text{ Hz}$, $J_{A,A'} \approx J_{X,X'}$)), 7.83 (s, 6H, **ArH**-triphenylene), 6.90 (d, 2H^X , **ArH**, XX' part of $\text{AA}'\text{XX}'$ spin system ($N_{A,X} = J_{A,X} + J_{A,X'} = 9.0 \text{ Hz}$, $J_{A,A'} \approx J_{X,X'}$)), 4.27-4.19

(m, 12H, OCH₂), 4.04 (t, 2H, ³J = 6.5 Hz, OCH₂), 3.88 (s, 3H, COOCH₃), 2.03-1.84 (m, 14H, OCH₂CH₂), 1.72-1.50 (m, 14H, OCH₂CH₂CH₂), 1.46-1.18 (m, 80H, rest of the CH₂ groups), 0.91-0.84 (m, 15H, CH₃). ¹³C{¹H} NMR (126 MHz, CDCl₃, Me₄Si): δ 166.84 (COO), 162.87 (O-C_{ar}), 149.02, 149.01, 148.98, 148.97, 148.95, 148.84 (O-C_{trif}), 131.54 (H^A-C_{ar}), 123.70, 123.66, 123.64, 123.57, 123.37 (C_{trif}), 122.37 (C_{ar}-COO), 114.01 (H^X-C_{ar}), 107.48, 107.46, 107.40, 107.37, 107.24 (H-C_{trif}), 69.79, 69.74, 69.71, 69.61, 69.52, 68.02 (O-CH₂), 51.78 (COO-CH₃), 31.93, 29.73, 29.71, 29.68, 29.55, 29.50, 29.38, 29.16, 26.22, 26.01, 25.90, 22.69 (-CH₂-), 14.11 (-CH₃).

4-[6-(3,6,7,10,11-pentadodecyloxytriphenylen-2-oxy)hexyloxy]benzoic acid

A mixture of 2-(6-((4-methoxycarbonyl)phenoxy)hexyloxy)-3,6,7,10,11-pentakis(dodecyloxy)triphenylene (3.25 g, 2.32 mmol) and NaOH (0.34g, 8.4 mmol) in 150 mL of ethanol, was refluxed for 2 hours. After cooling to room temperature, the reaction mixture was poured into 150 ml of water and acidified with HCl 0.1M. CH₂Cl₂ (70 mL) was added to this mixture and the organic layer was separated, dried over MgSO₄, and evaporated to dryness to give a yellow solid (3.10 g, 96 % yield). IR (ν, cm⁻¹): 3100-3600 (s, COO-H), 1684 (vs, C=O). ¹H NMR (500 MHz, CDCl₃): δ 8.05 (d, 2H^A, ArH, AA' part of AA'XX' spin system (N_{A,X} = J_{A,X} + J_{A,X'} = 9.0 Hz, J_{A,A'} ≈ J_{X,X'})), 7.84 (s, 6H, ArH-triphenylene), 6.93 (d, 2H^X, ArH, XX' part of AA'XX' spin system (N_{A,X} = J_{A,X} + J_{A,X'} = 9.0 Hz, J_{A,A'} ≈ J_{X,X'})), 4.28-4.19 (m, 12H, OCH₂), 4.06 (t, 2H, ³J = 6.5 Hz, OCH₂), 2.04-1.85 (m, 14H, OCH₂CH₂), 1.73-1.51 (m, 14H, OCH₂CH₂CH₂), 1.47-1.19 (m, 80H, rest of the CH₂ groups), 0.92-0.83 (m, 15H, CH₃). ¹³C{¹H} NMR (126 MHz, CDCl₃, Me₄Si): δ 171.37 (COOH), 163.59 (O-C_{ar}), 149.02, 149.01, 148.98, 148.97, 148.95, 148.83 (O-C_{trif}), 132.31 (H^A-C_{ar}), 123.71, 123.66, 123.65, 123.58, 123.57 (C_{trif}), 121.38 (C_{ar}-COO), 114.14 (H^X-C_{ar}), 107.49, 107.48, 107.41, 107.38, 107.25 (H-C_{trif}), 69.80, 69.75, 69.72,

69.71, 69.62, 69.52, 68.10 (O-CH₂), 31.93, 29.73, 29.70, 29.68, 29.38, 29.14, 26.21, 26.01, 25.89, 22.69 (-CH₂-), 14.11 (-CH₃).

2-(6-((4-((3-hydroxy-4-formyl)phenoxy)carbonyl)phenoxy)hexyloxy)-3,6,7,10,11-pentakis(dodecyloxy)triphenylene

To a solution of 2-(6-((4-carboxy)phenoxy)hexyloxy)-3,6,7,10,11-pentakis(dodecyloxy)triphenylene (3.10 g, 2.24 mmol) and 2,4-dihydroxybenzaldehyde (0.32 g, 2.24 mmol) in 150 mL of dry dichloromethane, were added N,N'-dicyclohexylcarbodiimide (DCC) (0.513 g, 2.46 mmol) and 4-dimethylaminopyridine (DMAP) (21 mg, 0.22 mmol). The mixture was stirred for 24 h at room temperature. The solvent was evaporated and the crude product was purified by column chromatography (silica gel with dichloromethane/hexane 2/1 as eluent) to give a white solid (2.50 g, 374 % yield). IR (ν , cm⁻¹) 1732 (s, C=O, ester), 1656 (s, C=O, aldehyde). ¹H NMR (500 MHz, CDCl₃): δ 11.25 (s, 1H, OH), 9.87 (s, 1H, CHO), 8.11 (d, 2H^A, ArH, AA' part of AA'XX' spin system ($N_{A,X} = J_{A,X} + J_{A,X'} = 8.9$ Hz, $J_{A,A'} \approx J_{X,X'}$)), 7.87-7.83 (m, 6H, ArH-triphenylene), 7.59 (d, 1H, ³J = 8.4 Hz, ArH⁵), 6.97 (d, 2H^X, ArH, XX' part of AA'XX' spin system ($N_{A,X} = J_{A,X} + J_{A,X'} = 8.9$ Hz, $J_{A,A'} \approx J_{X,X'}$)), 6.90 (dd, 1H, ³J = 8.4 Hz, ⁴J = 2.1 Hz, ArH⁶), 6.87 (d, 1H, ⁴J = 2.1 Hz, ArH²) 4.29-4.20 (m, 12H, OCH₂), 4.08 (t, 2H, ³J = 6.5 Hz, OCH₂), 2.04-1.87 (m, 14H, OCH₂CH₂), 1.74-1.52 (m, 14H, OCH₂CH₂CH₂), 1.47-1.21 (m, 80H, rest of the CH₂ groups), 0.92-0.84 (m, 15H, CH₃). ¹³C{¹H} NMR (126 MHz, CDCl₃, Me₄Si): δ 195.42 (CHO), 163.82 (COO), 163.81 (O-C_{ar}), 163.18 (C_{ar}-OH), 157.88 (COO-C_{ar}), 149.05, 149.03, 148.99, 148.95, 148.81 (O-C_{trif}), 134.87 (H⁵-C_{ar}), 132.44 (H^A-C_{ar} AA'XX'), 123.71, 123.68, 123.65, 123.56, 123.55 (C_{trif}), 120.78 (C_{ar}-COO), 118.56 (C_{ar}-CHO), 114.39 (H^X-C_{ar} AA'XX'), 114.12 (H⁶-C_{ar}), 110.85 (H²-C_{ar}), 107.53, 107.47, 107.41, 107.35, 107.33,

107.21 (H-C_{trif}), 69.82, 69.75, 69.71, 69.69, 69.59, 69.50, 68.22 (O-CH₂), 31.93, 29.74, 29.71, 29.68, 29.55, 29.49, 29.38, 29.11, 26.22, 26.00, 25.88, 22.69 (-CH₂-), 14.11 (-CH₃).

Synthesis of Schiff-base ligands

The Schiff-base ligands were synthesized by condensation of 2-(6-((4-((3-hydroxy-4-formyl)phenoxy)carbonyl)phenoxy)hexyloxy)-3,6,7,10,11-pentakis(dodecyloxy)triphenylene (1.00 g, 0.664 mmol) and the corresponding diamine (0.332 mmol) in absolute ethanol with acetic acid as catalyst. The diimines were purified by recrystallization from ethanol and isolated as yellow crystals.

N,N'-Bis-(2-hydroxy-4-(((4-(6-(3,6,7,10,11-pentakis(dodecyloxy)triphenylene-2-yl)oxy)hexyloxy)phenyl)oxycarbonyl)benzyl)ethane-1,2-diimine (1a).

Yield: 0.97 g (95%). IR (ν, cm⁻¹): 1733 (s, C=O, ester), 1630 (s, C=N). ¹H NMR (500 MHz, CDCl₃): δ 13.53 (br, 2H, OH), 8.35 (s, 2H, CHN), 8.12 (d, 4H^A, ArH, AA' part of AA'XX' spin system (N_{A,X} = J_{A,X} + J_{A,X'} = 9.0 Hz, J_{A,A'} ≈ J_{X,X'})), 7.84 (s, 12H, ArH-triphenylene), 7.27 (d, 2H, ³J = 8.4 Hz, ArH⁶), 6.96 (d, 4H^X, ArH, XX' part of AA'XX' spin system (N_{A,X} = J_{A,X} + J_{A,X'} = 9.0 Hz, J_{A,A'} ≈ J_{X,X'})), 6.81 (d, 2H, ⁴J = 2.2 Hz, ArH³), 6.74 (dd, 2H, ³J = 8.4 Hz, ⁴J = 2.2 Hz, ArH⁵), 4.28-4.20 (m, 24H, OCH₂), 4.08 (t, 4H, ³J = 6.4 Hz, OCH₂), 3.93 (s, 4H, NCH₂), 2.05-1.86 (m, 28H, OCH₂CH₂), 1.74-1.51 (m, 28H, OCH₂CH₂CH₂), 1.47-1.20 (m, 160H, rest of the CH₂ groups), 0.94-0.83 (m, 30H, CH₃). ¹³C{¹H} NMR (126 MHz, CDCl₃, Me₄Si): δ 165.83 (CHN), 164.33 (COO), 163.54 (O-C_{ar}), 162.57 (C_{ar}-OH), 154.29 (COO-C_{ar}), 149.03, 149.02, 148.99, 148.97, 148.96, 148.84 (O-C_{trif}), 132.35 (H⁶-C_{ar}), 132.33 (H^A-C_{ar} AA'XX'), 123.71, 123.66, 123.64, 123.57 (C_{trif}), 121.36 (C_{ar}-COO), 116.46 (C_{ar}-CHN), 114.26 (H^X-C_{ar} AA'XX'), 112.59 (H⁵-C_{ar}), 110.43 (H³-C_{ar}), 107.50, 107.47, 107.41, 107.37, 107.24 (H-C_{trif}), 69.81, 69.74, 69.72, 69.70, 69.62, 69.54, 68.18 (O-CH₂), 59.51 (CHN-CH₂), 31.93, 31.73, 30.68, 29.49, 29.38, 29.16,

26.21, 26.04, 25.92, 22.69 (-CH₂-), 14.11 (-CH₃). Elemental analysis for C₁₉₈H₃₀₈N₂O₂₀ (%): calculated C, 78.32; H, 10.26; N, 0.92; found C, 78.55; H, 10.58; N, 1.08. MS (MALDI-TOF): m/z calc. for [C₁₉₈H₃₀₈N₂O₂₀ (M⁺)]: 3034.3140; found 3034.3156.

N,N'-Bis-(2-hydroxy-4-(((4-(6-(3,6,7,10,11-pentakis(dodecyloxy)triphenylen-2-yl)oxy)hexyloxy)phenyl)oxycarbonyl)benzyl)propane-1,3-diimine (1b).

Yield: 0.85 g, (84%). IR (ν, cm⁻¹) 1737 (s, C=O, ester), 1634 (s, C=N). ¹H NMR (500 MHz, CDCl₃): δ 13.78 (s, 2H, OH), 8.37 (s, 2H, CHN), 8.13 (d, 4H^A, ArH, AA' part of AA'XX' spin system (N_{A,X} = J_{A,X} + J_{A,X'} = 9.0 Hz, J_{A,A'} ≈ J_{X,X'})), 7.84 (s, 12H, ArH-triphenylene), 7.28 (d, 2H, ³J = 8.4 Hz, ArH⁶), 6.97 (d, 4H^X, ArH, XX' part of AA'XX' spin system (N_{A,X} = J_{A,X} + J_{A,X'} = 9.0 Hz, J_{A,A'} ≈ J_{X,X'})), 6.83 (d, 2H, ⁴J = 2.2 Hz, ArH³), 6.75 (dd, 2H, ³J = 8.4 Hz, ⁴J = 2.2 Hz, ArH⁵), 4.28-4.19 (m, 24H, OCH₂), 4.08 (t, 4H, ³J = 6.5 Hz, OCH₂), 3.71 (t, 4H, ³J = 6.5 Hz, NCH₂), 2.13 (p, 2H, ³J = 6.5 Hz, NCH₂CH₂), 2.06-1.86 (m, 28H, OCH₂CH₂), 1.74-1.51 (m, 28H, OCH₂CH₂CH₂), 1.48-1.17 (m, 160H, CH₂), 0.94-0.81 (m, 30H, CH₃). ¹³C{¹H} NMR (126 MHz, CDCl₃, Me₄Si): δ 164.79 (CHN), 164.38 (COO), 163.56 (O-C_{ar}), 162.83 (C_{ar}-OH), 154.23 (COO-C_{ar}), 149.04, 149.02, 148.99, 148.97, 148.96, 148.84 (O-C_{trif}), 132.33 (H^A-C_{ar} AA'XX'), 132.11 (H⁶-C_{ar}), 123.71, 123.68, 123.66, 123.64, 123.56 (C_{trif}), 121.36 (C_{ar}-COO), 116.54 (C_{ar}-CHN), 114.27 (H^X-C_{ar} AA'XX'), 112.50 (H⁵-C_{ar}), 110.50 (H³-C_{ar}), 107.50, 107.48, 107.41, 107.37, 107.24 (H-C_{trif}), 69.81, 69.74, 69.71, 69.70, 69.61, 69.53, 68.18 (O-CH₂), 59.45 (CHN-CH₂), 31.59 (CHN-CH₂CH₂), 31.93, 31.73, 29.70, 29.68, 29.55, 29.49, 29.44, 29.38, 29.15, 26.21, 26.04, 25.91, 22.69 (-CH₂-), 14.11 (-CH₃). Elemental analysis for C₁₉₉H₃₁₀N₂O₂₀ (%): calculated C, 78.35; H, 10.24; N, 0.92; found C, 78.67; H, 10.44; N, 1.08. MS (MALDI-TOF): m/z calc. for [C₁₉₉H₃₁₀N₂O₂₀ (M⁺)]: 3048.3297; found 3048.3283.

N,N'-Bis-(2-hydroxy-4-(((4-(6-(3,6,7,10,11-pentakis(dodecyloxy)triphenylen-2-yl)oxy)hexyloxy)phenyl)oxycarbonyl)benzyl)-(2,2'-dimethyl)propane-1,3-diimine (1c).

Yield: 0.96 g (96%). IR (ν , cm^{-1}) 1736 (s, C=O, ester), 1633 (s, C=N). ^1H NMR (500 MHz, CDCl_3) δ 13.91 (s, 2H, OH), 8.33 (s, 2H, CHN), 8.13 (d, 4H^A, ArH, AA' part of AA'XX' spin system ($N_{A,X} = J_{A,X} + J_{A,X'} = 9.0$ Hz, $J_{A,A'} \approx J_{X,X'}$)), 7.84 (s, 12H, ArH-triphenylene), 7.29 (d, 2H, $^3J = 8.4$ Hz, ArH⁶), 6.97 (d, 4H^X, ArH, XX' part of AA'XX' spin system ($N_{A,X} = J_{A,X} + J_{A,X'} = 9.0$ Hz, $J_{A,A'} \approx J_{X,X'}$)), 6.83 (d, 2H, $^4J = 2.2$ Hz, ArH³), 6.75 (dd, 2H, $^3J = 8.4$ Hz, $^4J = 2.2$ Hz, ArH⁵) 4.28-4.19 (m, 24H, OCH₂), 4.08 (t, 4H, $^3J = 6.5$ Hz, OCH₂), 3.48 (s, 4H, NCH₂), 2.06-1.86 (m, 28H, OCH₂CH₂), 1.74-1.51 (m, 28H, OCH₂CH₂CH₂), 1.48-1.17 (m, 160H, CH₂), 1.09 (s, 6H, NCH₂CCH₃), 0.94-0.81 (m, 30H, CH₃). $^{13}\text{C}\{^1\text{H}\}$ NMR (126 MHz, CDCl_3 , Me_4Si) δ 165.09 (CHN), 164.40 (COO), 163.56 (O-C_{ar}), 162.97 (C_{ar}-OH), 154.28 (COO-C_{ar}), 149.04, 149.02, 148.99, 148.97, 148.96, 148.84 (O-C_{trif}), 132.34 (H^A-C_{ar} AA'XX'), 132.22 (H⁶-C_{ar}), 123.71, 123.66, 123.64, 123.57, 123.56 (C_{trif}), 121.36 (C_{ar}-COO), 116.53 (C_{ar}-CHN), 114.27 (H^X-C_{ar} AA'XX'), 112.50 (H⁵-C_{ar}), 110.50 (H³-C_{ar}), 107.50, 107.47, 107.41, 107.37, 107.24 (H-C_{trif}), 69.81, 69.74, 69.71, 69.70, 69.61, 69.53, 68.18 (O-CH₂), 67.79 (CHN-CH₂), 36.25 (CHN-CH₂C-), 31.93, 29.73, 29.70, 29.68, 29.54, 29.49, 29.44, 29.38, 29.15, 26.21, 26.03, 25.91, 22.69 (-CH₂-), 24.33 (CHN-CH₂C-CH₃), 14.11 (-CH₃). Elemental analysis for $\text{C}_{201}\text{H}_{314}\text{N}_2\text{O}_{20}$ (%): calculated C, 78.42; H, 10.28; N, 0.91; found C, 78.55; H, 10.54; N, 1.01. MS (MALDI-TOF): m/z calc. for [$\text{C}_{201}\text{H}_{314}\text{N}_2\text{O}_{20}$ (M^+)]: 3076.3610; found 3076.3612.

Synthesis of the metal Schiff-base complexes

Nickel(II) and copper(II) complexes

A solution of the appropriate metal salt ($\text{Ni}(\text{OAc})_2 \cdot 4\text{H}_2\text{O}$ or $\text{Cu}(\text{OAc})_2 \cdot \text{H}_2\text{O}$) (0.058 mmol) in absolute ethanol (20 mL) was added dropwise to a stirred solution of the corresponding Schiff-base (0.058 mmol) in toluene (20 mL). The mixture was heated under reflux for 3 h. Upon cooling, the resulting precipitate was filtered off and purified by recrystallization from toluene/ethanol. The nickel complexes can also be purified by column chromatography (silica, ethyl acetate/hexane 1:1).

Nickel complexes

2a. Orange solid. Yield: 132 mg (74 %). IR (ν , cm^{-1}) 1732 (s, C=O, ester), 1616 (s, C=N). ^1H NMR (500 MHz, CDCl_3) δ 8.11 (d, 4H^{A} , ArH, AA' part of AA'XX' spin system ($N_{\text{A,X}} = J_{\text{A,X}} + J_{\text{A,X'}} = 9.0 \text{ Hz}$, $J_{\text{A,A'}} \approx J_{\text{X,X'}}$), 7.84 (s, 12H, ArH-triphenylene), 7.17 (s, 2H, CHN), 6.97 (d, 4H^{X} , ArH, XX' part of AA'XX' spin system ($N_{\text{A,X}} = J_{\text{A,X}} + J_{\text{A,X'}} = 9.0 \text{ Hz}$, $J_{\text{A,A'}} \approx J_{\text{X,X'}}$), 6.76 (d, 2H, $^3J = 8.4 \text{ Hz}$, ArH⁶), 6.61 (d, 2H, $^4J = 2.2 \text{ Hz}$, ArH³), 6.19 (dd, 2H, $^3J = 8.4 \text{ Hz}$, $^4J = 2.2 \text{ Hz}$, ArH⁵) 4.29-4.17 (m, 24H, OCH₂), 4.08 (t, 4H, $^3J = 6.5 \text{ Hz}$, OCH₂), 3.54 (br, 4H, NCH₂), 2.05-1.84 (m, 28H, OCH₂CH₂), 1.74-1.49 (m, 28H, OCH₂CH₂CH₂), 1.47-1.17 (m, 160H, CH₂), 0.93-0.80 (m, 30H, CH₃). $^{13}\text{C}\{^1\text{H}\}$ NMR (126 MHz, CDCl_3 , Me_4Si) δ 164.91 (COO), 164.89 (C_{ar}-O-Ni), 163.46 (O-C_{ar}), 161.37 (CHN), 155.08 (COO-C_{ar}), 149.03, 149.01, 148.98, 148.97, 148.96, 148.84 (O-C_{trif}), 132.49 (H⁶-C_{ar}), 132.37 (H^A-C_{ar} AA'XX'), 123.71, 123.66, 123.64, 123.57 (C_{trif}), 121.68 (C_{ar}-COO), 119.09 (C_{ar}-CHN), 114.24 (H^X-C_{ar} AA'XX'), 112.63 (H³-C_{ar}), 109.25 (H⁵-C_{ar}), 107.50, 107.47, 107.41, 107.37, 107.25 (H-C_{trif}), 69.80, 69.74, 69.72, 69.70, 69.62, 69.55, 68.21 (O-CH₂), 58.41 (CHN-CH₂), 31.93, 31.91, 30.90, 29.73, 29.70, 29.67, 29.54, 29.49, 29.38, 29.20, 26.21, 26.09, 25.97, 22.69 (-CH₂-), 14.11 (-CH₃). Elemental analysis for $\text{C}_{198}\text{H}_{306}\text{N}_2\text{NiO}_{20}$ (%): calculated C, 76.88; H, 9.97; N, 0.91; found C, 77.14; H, 10.30; N, 1.05. MS (MALDI-TOF): m/z calc. for $[\text{C}_{198}\text{H}_{306}\text{N}_2\text{NiO}_{20} (\text{M}^+)]$: 3091.2371; found: 3091.2563.

2b. Yellowish solid. Yield: 114 mg (64 %). IR (ν , cm^{-1}) 1728 (s, C=O), 1615 (s, C=N). ^1H NMR (500 MHz, CDCl_3) δ 8.10 (d, 4H^{A} , ArH, AA' part of AA'XX' spin system ($N_{\text{A,X}} = J_{\text{A,X}} + J_{\text{A,X'}} = 9.0 \text{ Hz}$, $J_{\text{A,A'}} \approx J_{\text{X,X'}}$), 7.84 (s, 12H, ArH-triphenylene), 7.09 (s, 2H, CHN), 6.96 (d, 4H^{X} , ArH, XX' part of AA'XX' spin system ($N_{\text{A,X}} = J_{\text{A,X}} + J_{\text{A,X'}} = 9.0 \text{ Hz}$, $J_{\text{A,A'}} \approx J_{\text{X,X'}}$), 6.87 (d, 2H, $^3J = 8.4 \text{ Hz}$, ArH⁶), 6.67 (d, 2H, $^4J = 2.2 \text{ Hz}$, ArH³), 6.27 (dd, 2H, $^3J = 8.4 \text{ Hz}$, $^4J = 2.2 \text{ Hz}$, ArH⁵) 4.31-4.18 (m, 24H, OCH₂), 4.07 (t, 4H, $^3J = 6.5 \text{ Hz}$, OCH₂), 3.56 (t, 4H, $^3J = 6.5 \text{ Hz}$, NCH₂), 2.04-1.85 (m, 30H, OCH₂CH₂ and NCH₂CH₂), 1.74-1.51 (m, 28H, OCH₂CH₂CH₂), 1.48-1.17 (m,

160H, CH₂), 0.94-0.81 (m, 30H, CH₃). ¹³C{¹H} NMR (126 MHz, CDCl₃, Me₄Si) δ 164.76 (C_{ar}-O-Ni), 164.52 (COO), 163.86 (CHN), 163.38 (O-C_{ar}), 155.37 (COO-C_{ar}), 149.01, 149.00, 148.97, 148.95, 148.84 (O-C_{trif}), 133.67 (H⁶-C_{ar}), 132.26 (H^A-C_{ar} AA'XX'), 123.69, 123.64, 123.63, 123.56 (C_{trif}), 121.71 (C_{ar}-COO), 118.36 (C_{ar}-CHN), 114.18 (H^X-C_{ar} AA'XX'), 112.64 (H³-C_{ar}), 109.36 (H⁵-C_{ar}), 107.46, 107.36, 107.24 (H-C_{trif}), 69.78, 69.72, 69.70, 69.61, 69.54, 68.17 (O-CH₂), 56.11 (CHN-CH₂), 31.91, 29.72, 29.69, 29.66, 29.53, 29.48, 29.36, 29.18, 26.20, 26.07, 25.94, 22.67 (-CH₂-), 25.82 (CHN-CH₂-CH₂), 14.10 (-CH₃). Elemental analysis for C₁₉₉H₃₀₈N₂NiO₂₀ (%): calculated C, 76.92; H, 9.99; N, 0.90; found C, 76.73; H, 10.02; N, 0.96. MS (MALDI-TOF): m/z calc. for [C₁₉₉H₃₀₈N₂NiO₂₀ (M+Na)⁺]: 3127,2391; found: 3127,2615.

2c. Yellowish solid. Yield: 102 mg (57 %). IR (ν, cm⁻¹) 1729 (s, C=O), 1616 (s, C=N). ¹H NMR (500 MHz, CDCl₃) δ 8.10 (d, 4H^A, ArH, AA' part of AA'XX' spin system (N_{A,X} = J_{A,X} + J_{A,X'} = 8.8 Hz, J_{A,A'} ≈ J_{X,X'})), 7.84 (s, 12H, ArH-triphenylene), 7.07 (s, 2H, CHN), 7.00 (d, 2H, ³J = 8.5 Hz, ArH⁶), 6.95 (d, 4H^X, ArH, XX' part of AA'XX' spin system (N_{A,X} = J_{A,X} + J_{A,X'} = 8.8 Hz, J_{A,A'} ≈ J_{X,X'})), 6.77 (d, 2H, ⁴J = 2.2 Hz, ArH³), 6.36 (dd, 2H, ³J = 8.5 Hz, ⁴J = 2.2 Hz, ArH⁵) 4.29-4.18 (m, 24H, OCH₂), 4.07 (t, 4H, ³J = 6.5 Hz, OCH₂), 3.31 (s, 4H, NCH₂), 2.03-1.87 (m, 28H, OCH₂CH₂ and NCH₂CH₂), 1.76-1.11 (m, 188H, CH₂), 0.93 (s, 6H, CH₃) 0.92-0.82 (m, 30H, CH₃). ¹³C{¹H} NMR (126 MHz, CDCl₃, Me₄Si) δ 165.20 (C_{ar}-O-Ni), 164.33 (COO), 163.53 (CHN), 163.39 (O-C_{ar}), 155.65 (COO-C_{ar}), 149.03, 149.02, 148.99, 148.97, 148.87 (O-C_{trif}), 133.36 (H⁶-C_{ar}), 132.30 (H^A-C_{ar} AA'XX'), 123.71, 123.65, 123.59 (C_{trif}), 121.72 (C_{ar}-COO), 118.35 (C_{ar}-CHN), 114.19 (H^X-C_{ar} AA'XX'), 113.16 (H³-C_{ar}), 109.84 (H⁵-C_{ar}), 107.48, 107.39, 107.27 (H-C_{trif}), 69.79, 69.74, 69.72, 69.63, 69.56, 68.17 (O-CH₂), 68.61 (CHN-CH₂), 33.88 (CHN-CH₂C-), 31.93, 29.73, 29.70, 29.68, 29.55, 29.49, 29.47, 29.38, 26.20, 26.21, 20.08, 25.96, 22.69 (-CH₂-), 25.28 (CHN-CH₂C-CH₃), 14.11 (-CH₃). Elemental analysis for C₂₀₁H₃₁₂N₂NiO₂₀ (%): calculated C, 77.00; H, 10.03; N, 0.89; found C, 76.79; H, 10.02; N, 0.93. MS (MALDI-TOF): m/z calc. for [C₂₀₁H₃₁₂N₂NiO₂₀ (M⁺)]: 3132.2806; found: 3132.2889

Copper complexes

3a. Gray-purple solid. Yield: 128 mg (72 %). IR (ν , cm^{-1}) 1728 (s, C=O), 1615 (s, C=N). Elemental analysis for $\text{C}_{198}\text{H}_{306}\text{N}_2\text{CuO}_{20}$ (%): calculated C, 76.76; H, 9.96; N, 0.90; found C, 77.16; H, 10.12; N, 1.06. MS (MALDI-TOF): m/z calc. for $[\text{C}_{198}\text{H}_{306}\text{N}_2\text{CuO}_{20} (\text{M}^+)]$: calc.: 3096.2313; found: 3096.1987.

3b. Green solid. Yield: 168 mg (94 %). IR (ν , cm^{-1}) 1728 (s, C=O), 1616 (s, C=N). Elemental analysis for $\text{C}_{199}\text{H}_{308}\text{N}_2\text{CuO}_{20}$ (%): calculated C, 76.80; H, 9.98; N, 0.90; found C, 76.52; H, 10.08; N, 0.96. MS (MALDI-TOF): m/z calc. for $[\text{C}_{199}\text{H}_{308}\text{N}_2\text{CuO}_{20} (\text{M}^+)]$: calc.: 3109,2436; found: 3109,2447.

3c. Green solid. Yield: 157 mg (88 %). IR (ν , cm^{-1}) 1729 (s, C=O), 1616 (s, C=N). Elemental analysis for $\text{C}_{201}\text{H}_{312}\text{N}_2\text{CuO}_{20}$ (%): calculated C, 76.88; H, 10.02; N, 0.89; found C, 76.49; H, 10.05; N, 0.93. MS (MALDI-TOF): m/z calc. for $[\text{C}_{201}\text{H}_{312}\text{N}_2\text{CuO}_{20} (\text{M}^+)]$: 3137,2749; found: 3137,2774.

Oxovanadium(IV) complexes

A solution of $\text{VOSO}_4 \cdot 5\text{H}_2\text{O}$ (14.59 mg, 0.058 mmol) in methanol (15 mL) was added dropwise to a stirred solution of the corresponding Schiff-base **H₂L** (0.058 mmol) and triethylamine (0.016 mL, 0.116 mmol) in toluene (20 mL). The mixture was heated under reflux for 4 h. Then, the solvent was removed under reduced pressure to yield the product that was recrystallized in toluene/ethanol.

4a. Green solid. Yield: 0.078 g (44 %). IR (ν , cm^{-1}) 1732 (s, C=O), 1616 (s, C=N), 983 (s, V=O). Elemental analysis for $\text{C}_{198}\text{H}_{306}\text{N}_2\text{VO}_{21}$ (%): calculated C, 76.68; H, 9.94; N, 0.90; found C, 76.24; H, 10.03; N, 1.06. MS (MALDI-TOF): m/z calc. for $[\text{C}_{198}\text{H}_{306}\text{N}_2\text{VO}_{21} (\text{M}^+)]$: calc.: 3099.2373; found: 3099.2796.

4b. Yellowish solid. Yield: 0.144 g (80 %). IR (ν , cm^{-1}) 1732 (s, C=O), 1616 (s, C=N), 857 (s, V=O). Elemental analysis for $\text{C}_{199}\text{H}_{308}\text{N}_2\text{VO}_{21}$ (%): calculated C, 76.72; H, 9.96; N, 0.90; found C, 76.62; H, 10.25; N, 0.98. MS (MALDI-TOF): m/z calc. for $[\text{C}_{199}\text{H}_{308}\text{N}_2\text{VO}_{21} (\text{M}^+)]$: 3113.2639; found: 3113.2595

4c. Yellowish solid. Yield: 0.123 g (76 %). IR (ν , cm^{-1}) 1732 (s, C=O), 1618 (s, C=N), 871 (s, V=O). Elemental analysis for $\text{C}_{201}\text{H}_{312}\text{N}_2\text{VO}_{21}$ (%): calculated C, 76.80; H, 10.00; N, 0.89; found C, 76.64; H, 10.26; N, 0.99. MS (MALDI-TOF): m/z calc. for $[\text{C}_{201}\text{H}_{312}\text{N}_2\text{VO}_{21} (\text{M}^+)]$: 3141,2842; found: 3141,2824.

Table S1. UV-Visible data for the Schiff bases and their metal complexes, in dichloromethane solution at 298 K (10^{-5} M).

Compd.	λ /nm (ϵ / mol ⁻¹ cm ⁻¹)
1a	341 (9860), 309 (69915), 279 (268706), 269 (209049), 260 (153475)
1b	342 (8269), 309 (64857), 279 (250264), 270 (198458), 261 (147050)
1c	345 (16890), 309 (66347), 279 (255981), 271 (210570), 261 (163541)
2a	407 (8124), 342 (17736), 308 (69753), 279 (280796), 269 (232741), 260 (181417)
2b	411 (6420), 346 (15210), 307 (63113), 279 (274281), 271 (226477), 261 (166722)
2c	413 (8163), 346 (16327), 308 (67221), 279 (289266), 272 (244597), 261 (183423)
3a	566 (385),* 348 (19073), 304 (64928), 280 (284221), 269 (198935), 260 (162073)
3b	610 (196),* 348 (16866), 306 (62047), 279 (269246), 269 (195852), 260 (149649)
3c	613 (256),* 348 (16866), 306 (62047), 279 (269246), 269 (195852), 260 (149649)
4a	583 (166),* 347 (15845), 305 (75509), 280 (261447), 269 (194349), 260 (151704)
4b	574 (50),* 347 (15786), 309 (59869), 279 (257250), 271 (199167), 261 (152602)
4c	568 (59),* 347 (17113), 310 (59053), 279 (263909), 271 (198427), 262 (158267)

* Absorption bands observed in 10^{-4} M solutions.

¹H NMR spectra [Varian 500 (500.0 MHz)] in CDCl₃.

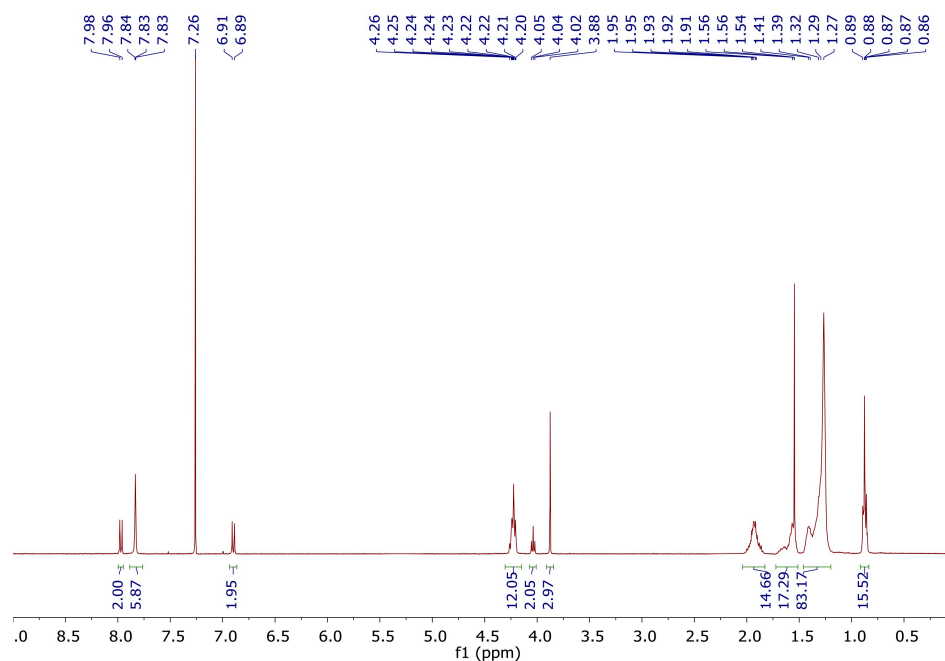


Figure S1: ¹H NMR spectrum of methyl 4-[6-(3,6,7,10,11-pentadecyloxytriphenylen-2-oxy)hexyloxy]benzoate.

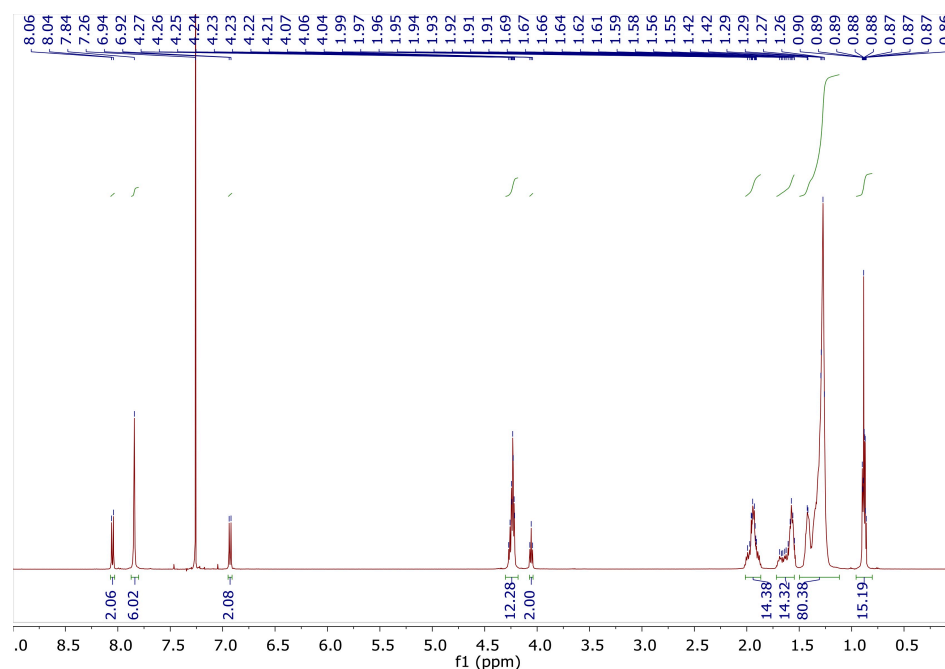


Figure S2: ¹H NMR spectrum of 4-[6-(3,6,7,10,11-pentadecyloxytriphenylen-2-oxy)hexyloxy]benzoic acid.

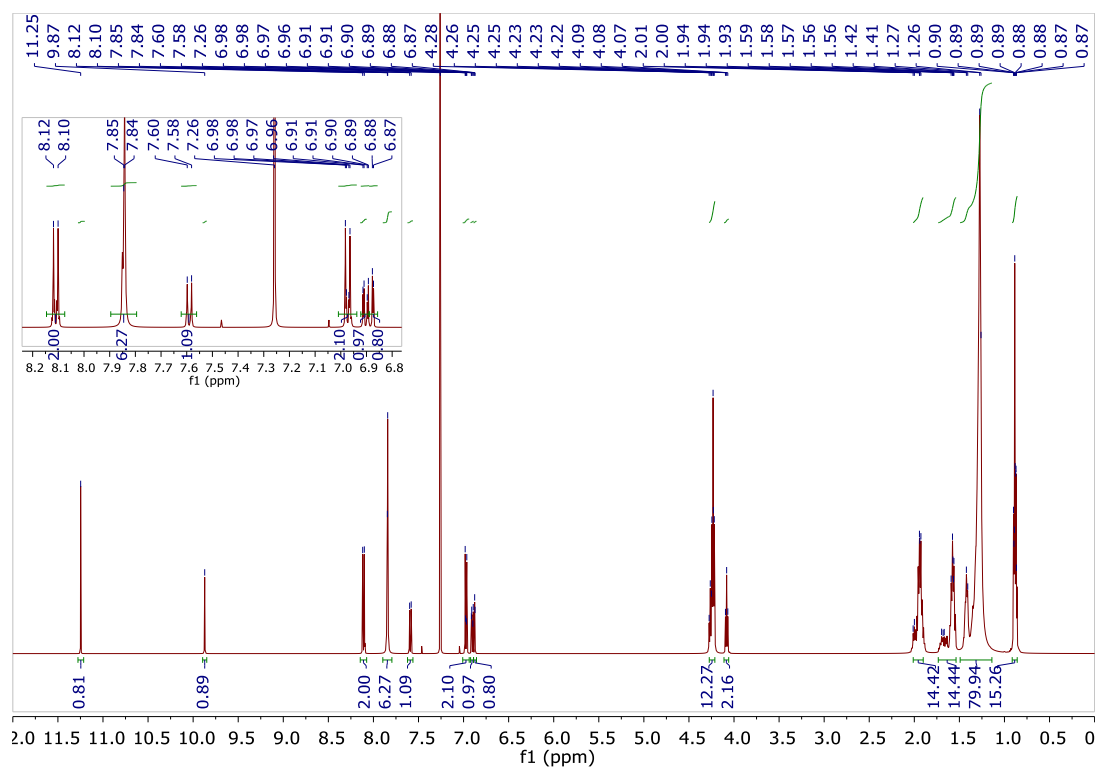


Figure S3: ¹H NMR spectrum of 2-((6-((4-(-hydroxy-4-formyl)phenoxy)carbonyl)phenoxy)hexyloxy)-3,6,7,10,11-pentakis(dodecyloxy)triphenylene.

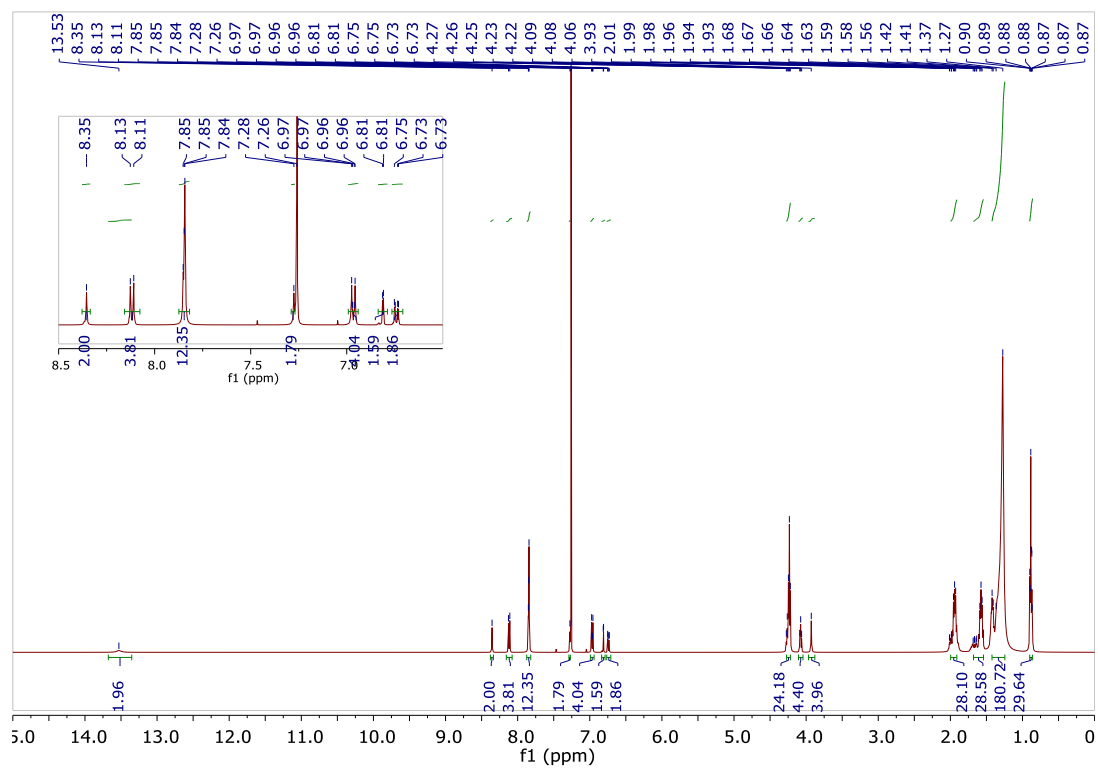


Figure S4: ¹H NMR spectrum of the free ligand Salen (1a).

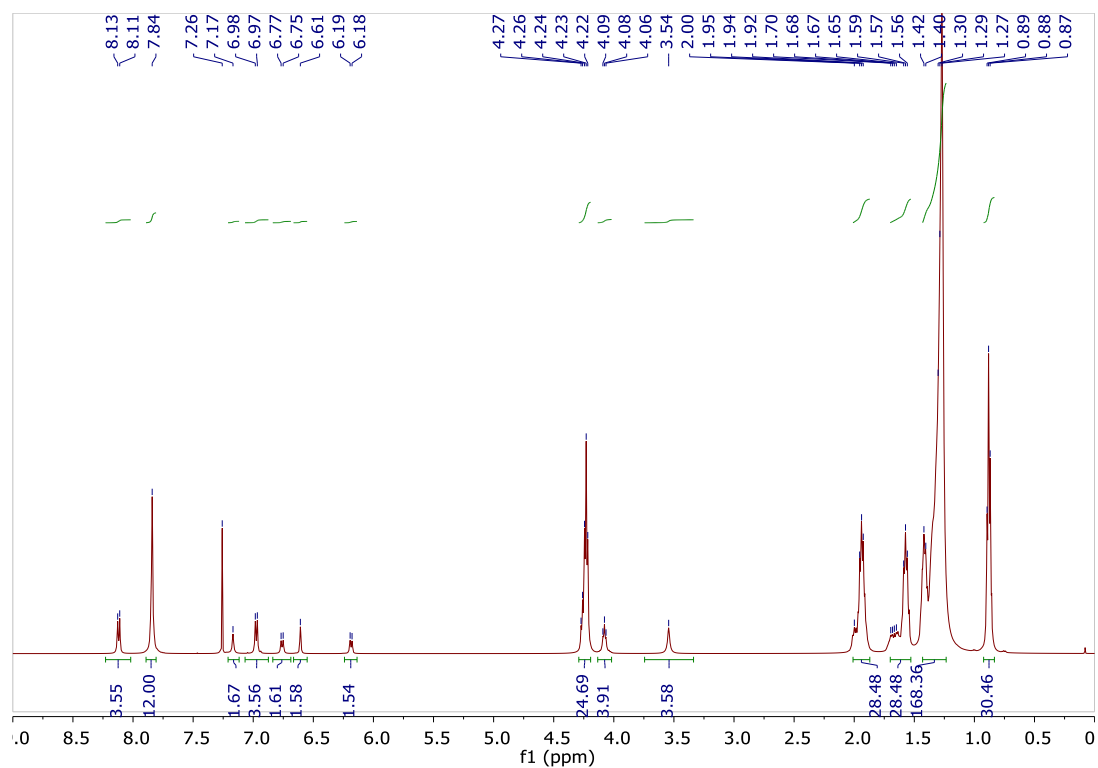


Figure S5: ¹H NMR spectrum of the complex **2a**.

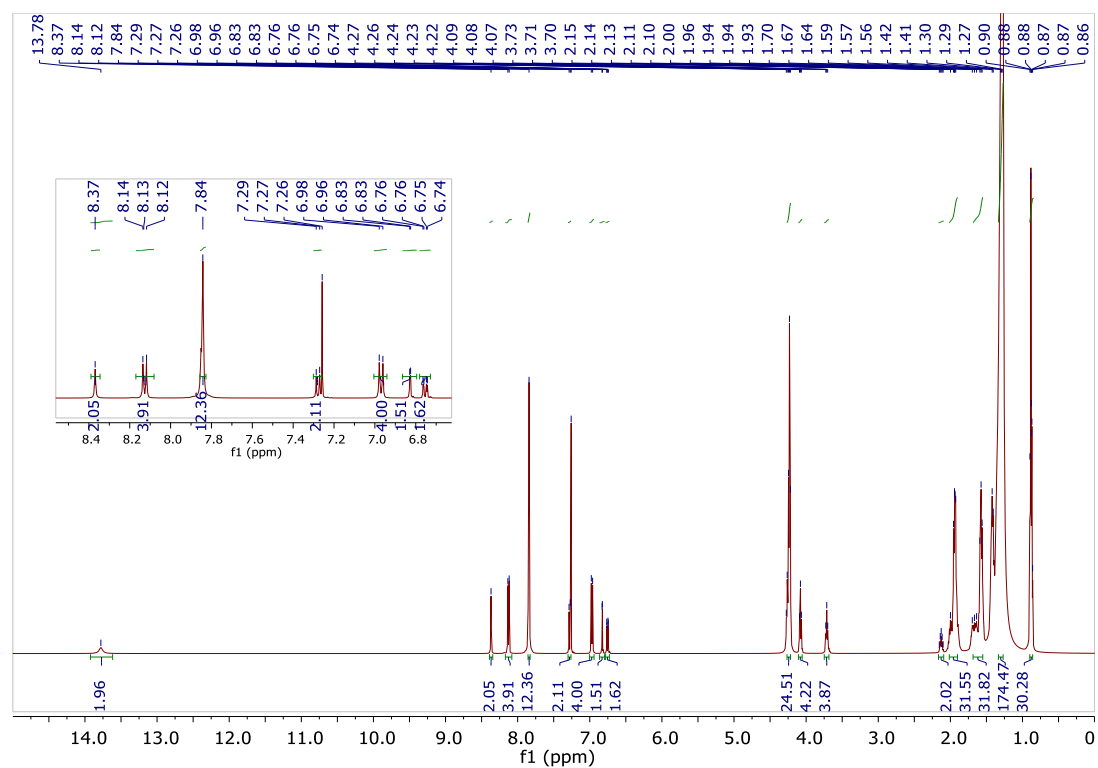


Figure S6: ¹H NMR spectrum of the free ligand **Salpn (1b)**.

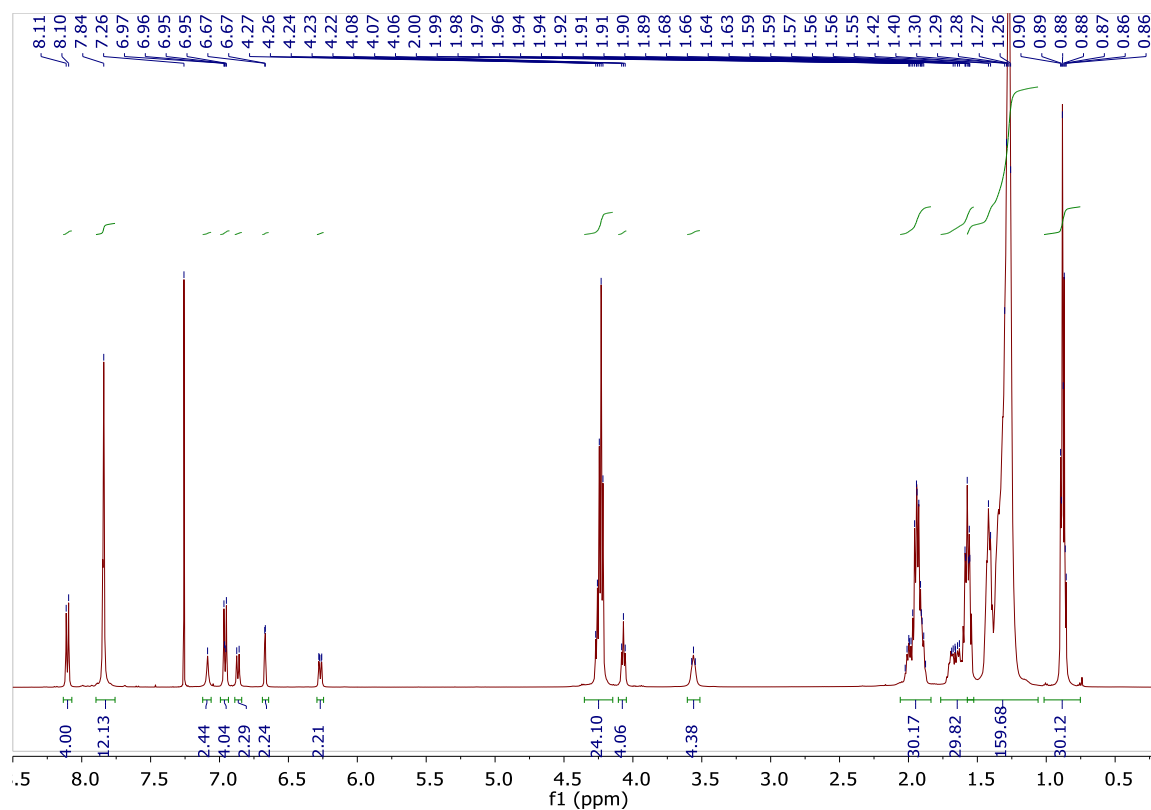


Figure S7: ^1H NMR spectrum of complex **2b.**

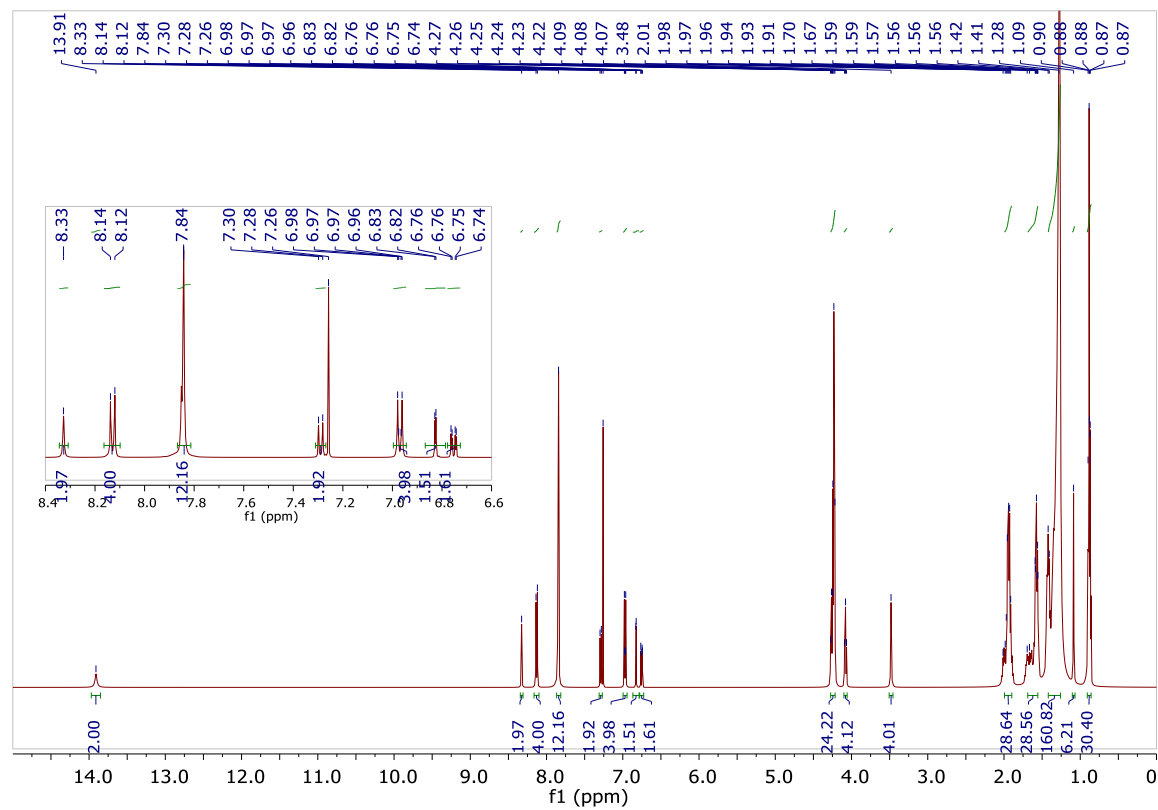


Figure S8: ^1H NMR spectrum of the free ligand **Me₂Salpn (1c).**

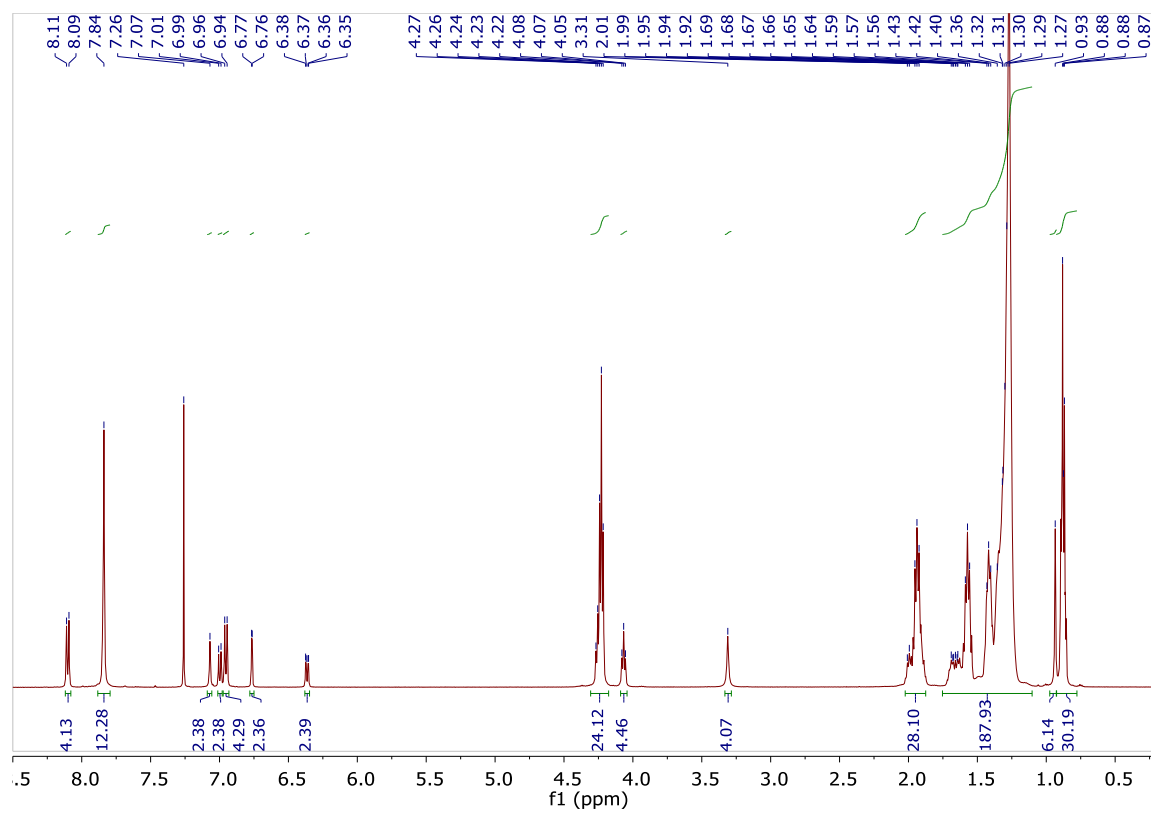


Figure S9: ^1H NMR spectrum of the complex **2c**.

^{13}C NMR spectra [Varian 500 (126.0 MHz)] in CDCl_3 .

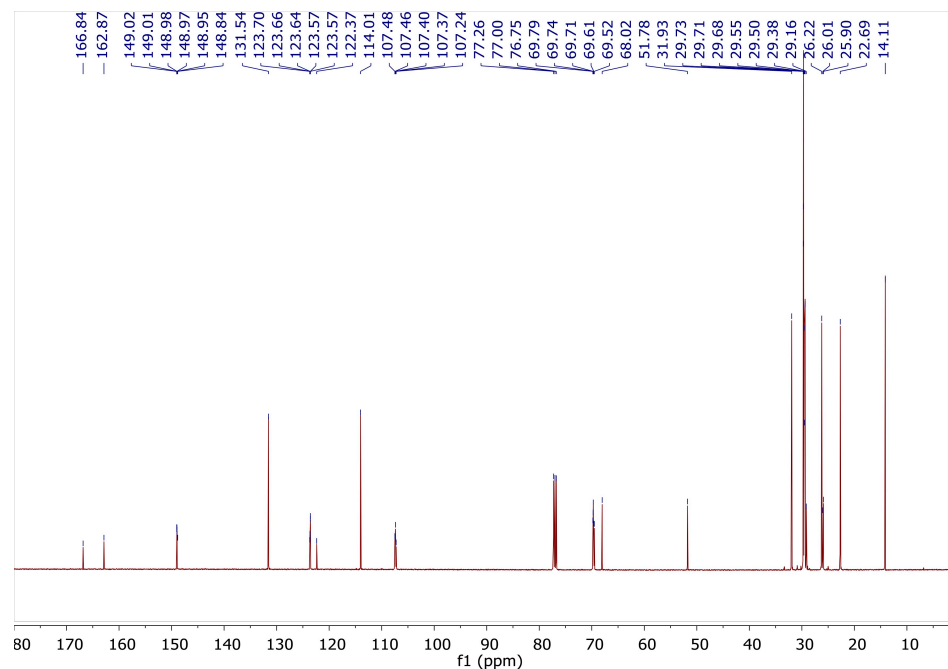


Figure S10: ^{13}C NMR spectrum of methyl 4-[6-(3,6,7,10,11-pentadecyloxytriphenylen-2-oxy)hexyloxy]benzoate.

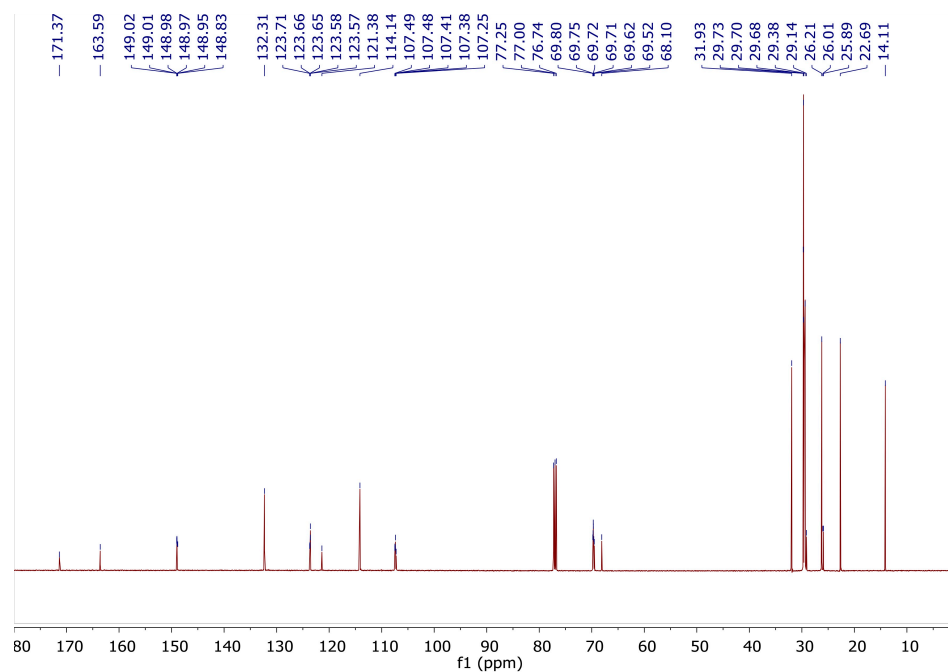


Figure S11: ^{13}C NMR spectrum of 4-[6-(3,6,7,10,11-pentadecyloxytriphenylen-2-oxy)hexyloxy]benzoic acid.

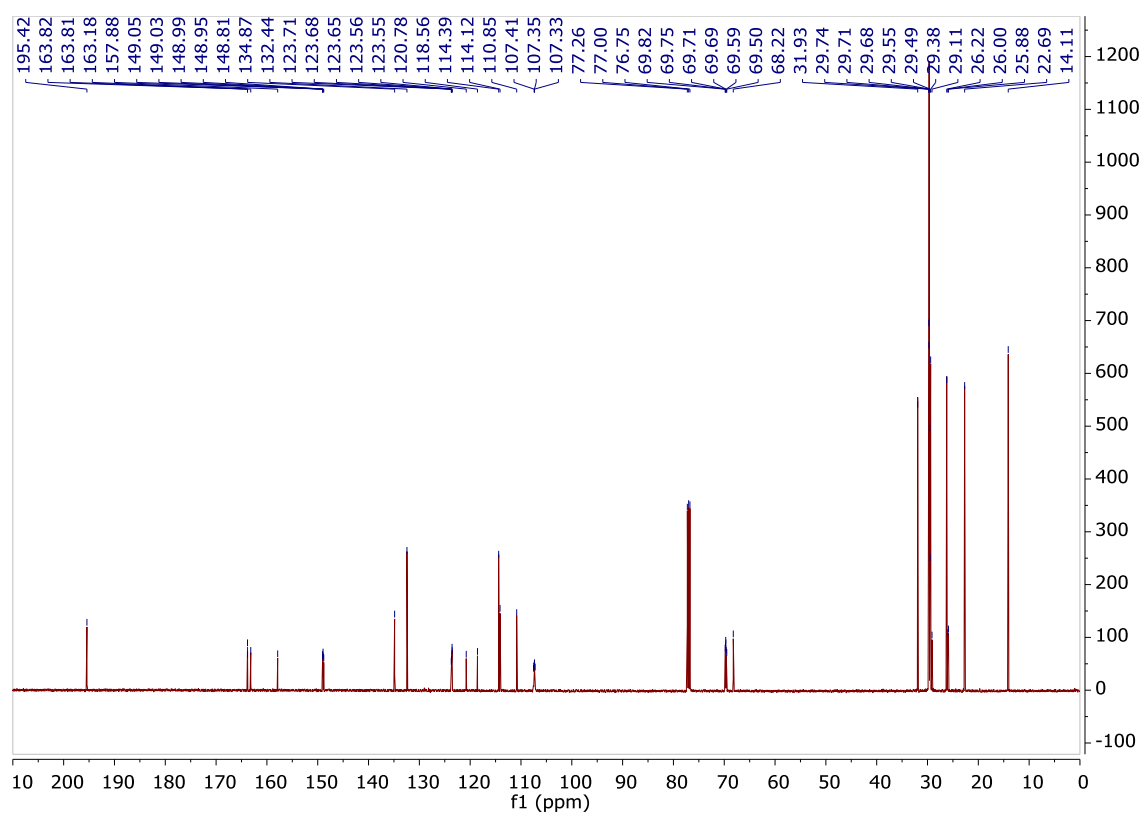


Figure S12: ^{13}C NMR spectrum of 2-(6-((4-(-hydroxy-4-formyl)phenoxy)carbonyl)phenoxy)hexyloxy)-3,6,7,10,11-pentakis(dodecyloxy)triphenylene.

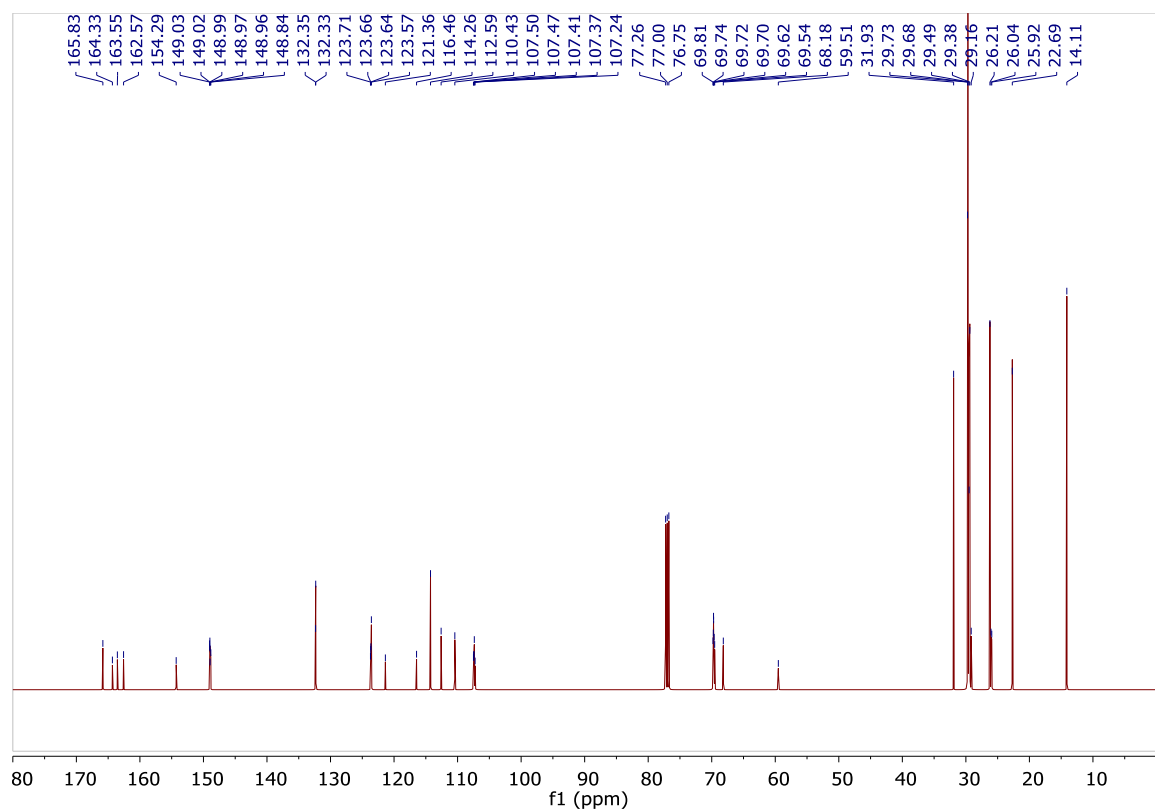


Figure S13: ^{13}C NMR spectrum of the free ligand Salen (**1a**).

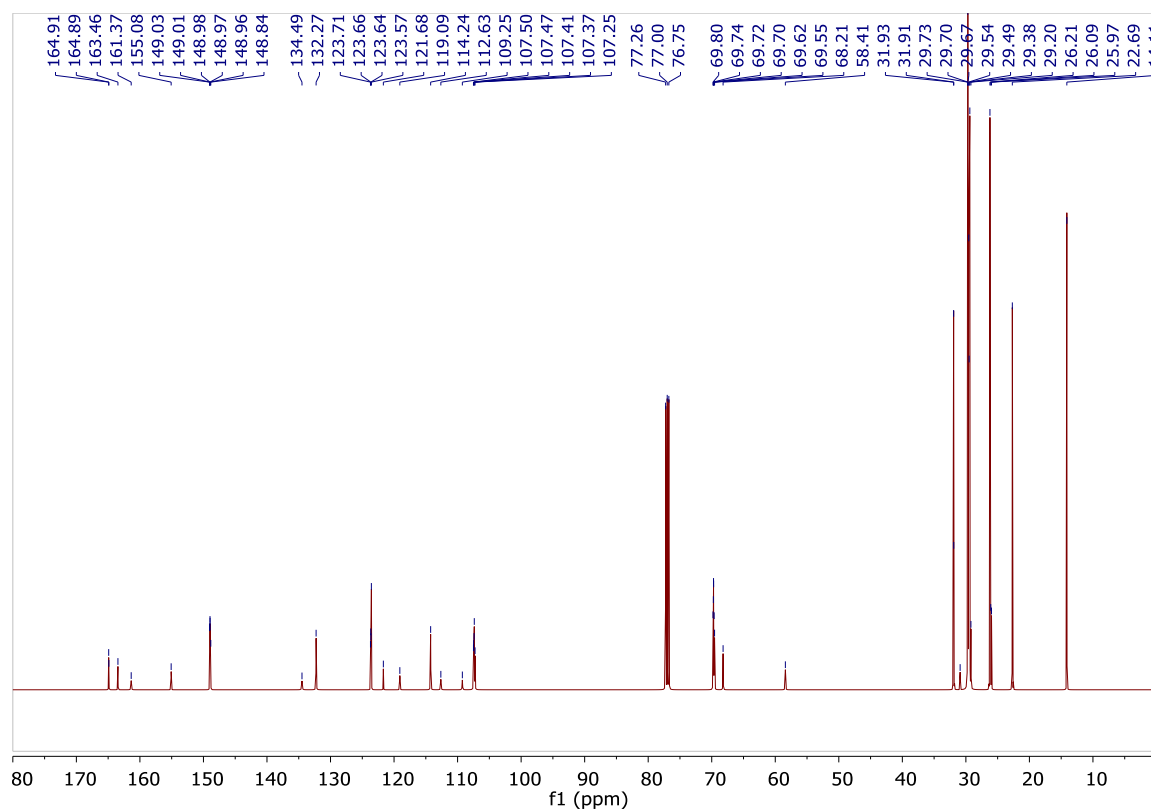


Figure S14: ^{13}C NMR spectrum of the complex **2a**.

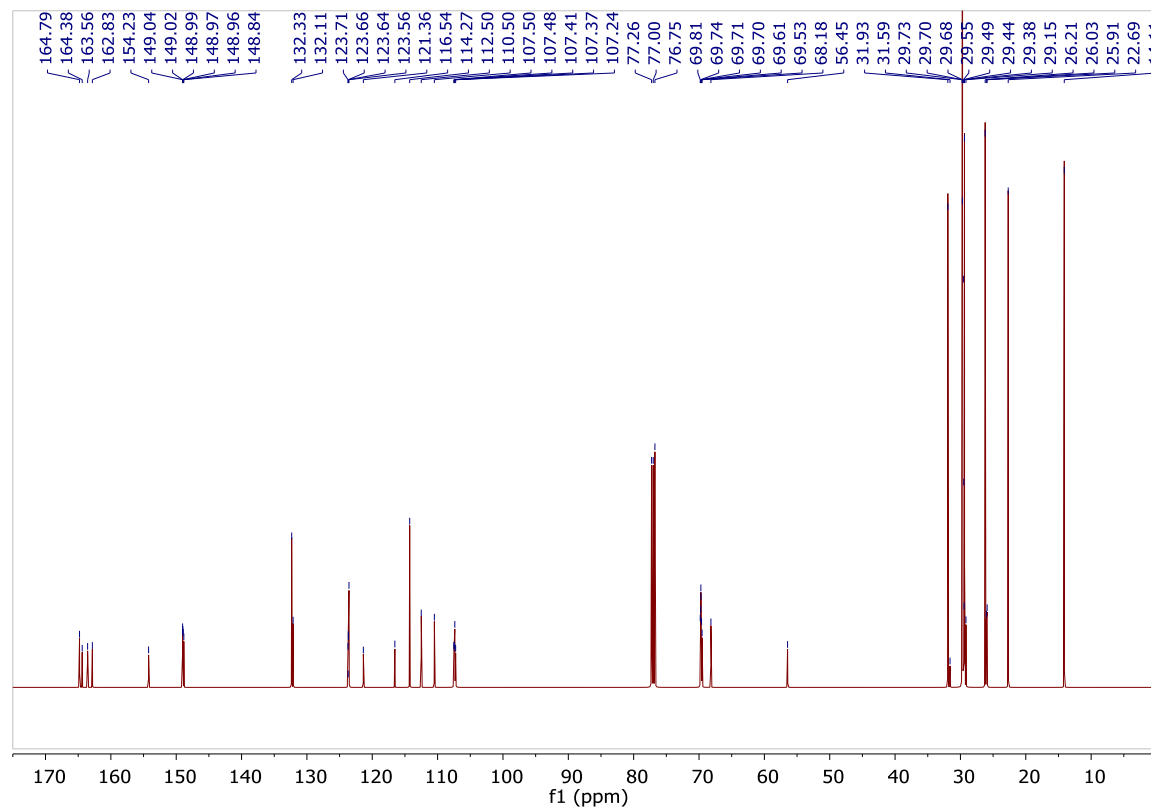


Figure S15: ^{13}C NMR spectrum of the free ligand Salpn (**1b**).

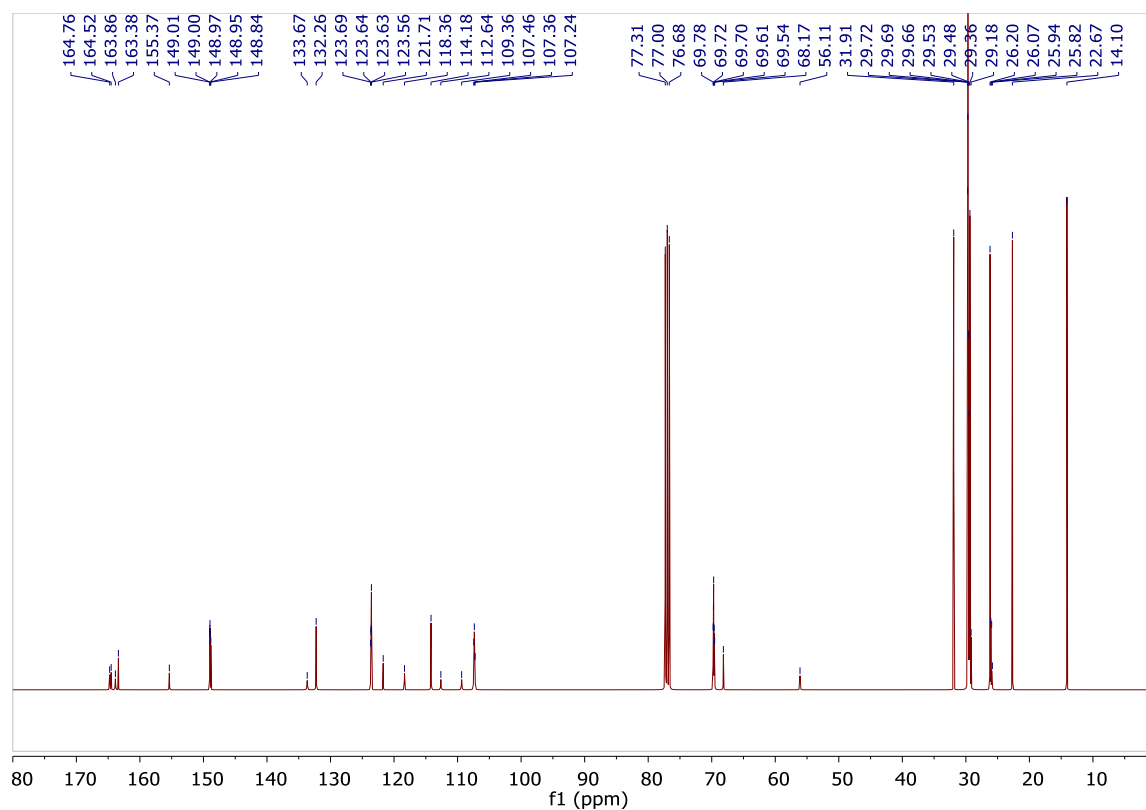


Figure S16: ^{13}C NMR spectrum of the complex **2b**.

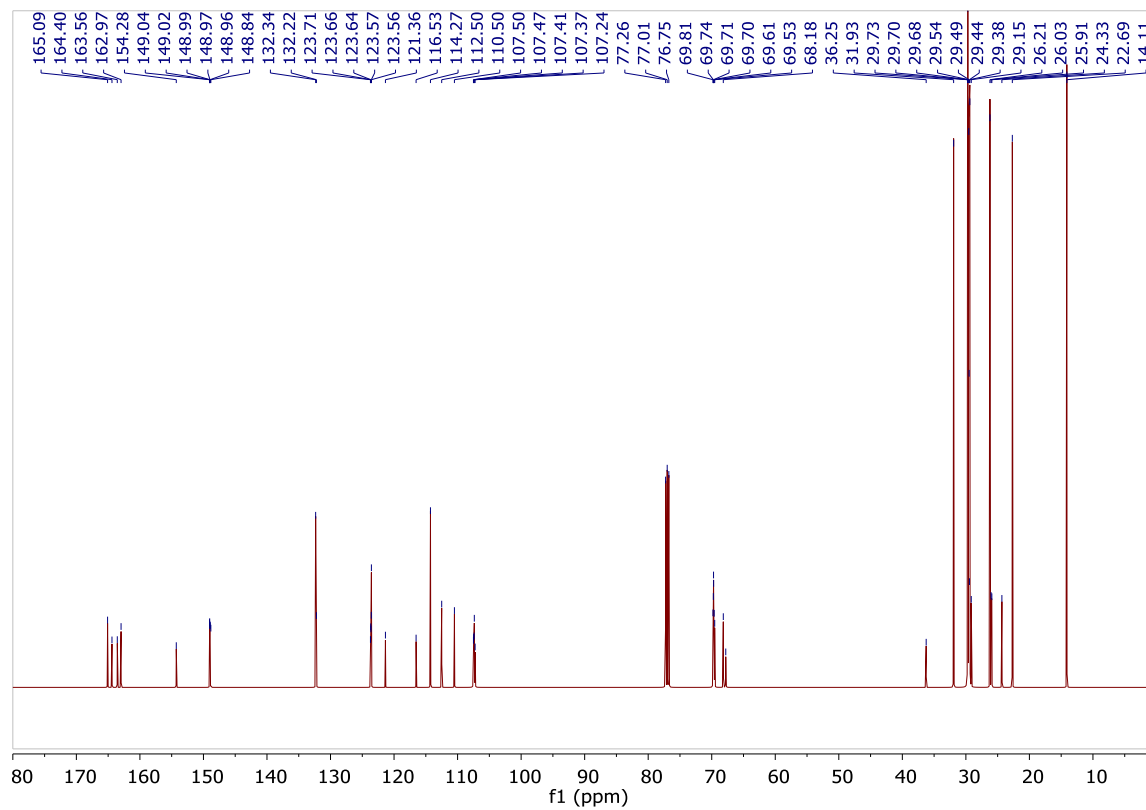


Figure S17: ^{13}C NMR spectrum of the free ligand Me₂Salpn (**1c**).

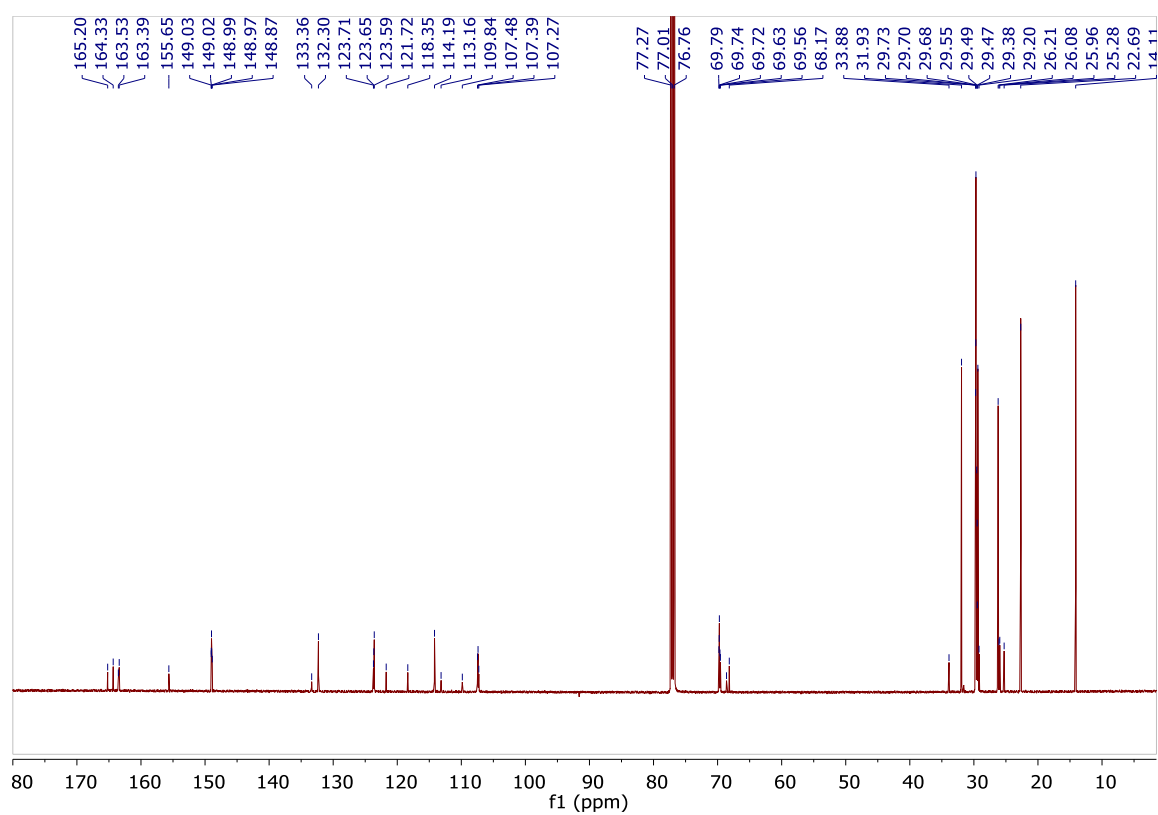


Figure S18: ^{13}C NMR spectrum of the complex **2c**.

MALDI-TOF MS

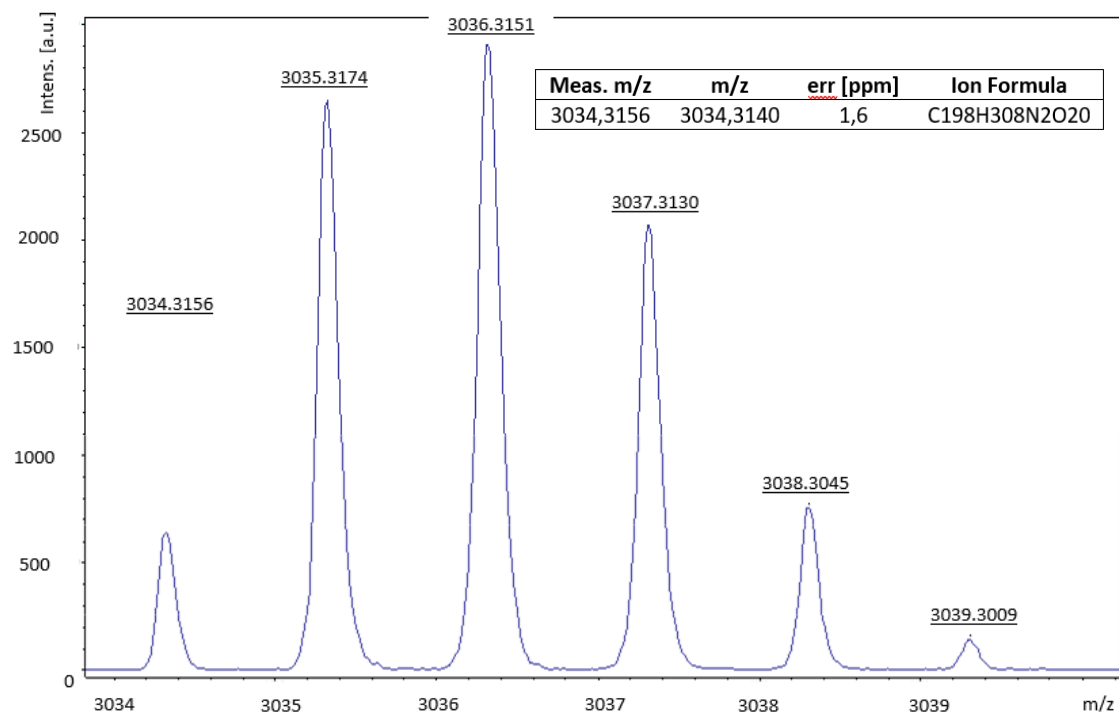


Figure S19: MALDI-TOF mass spectrum of the free ligand Salen (**1a**).

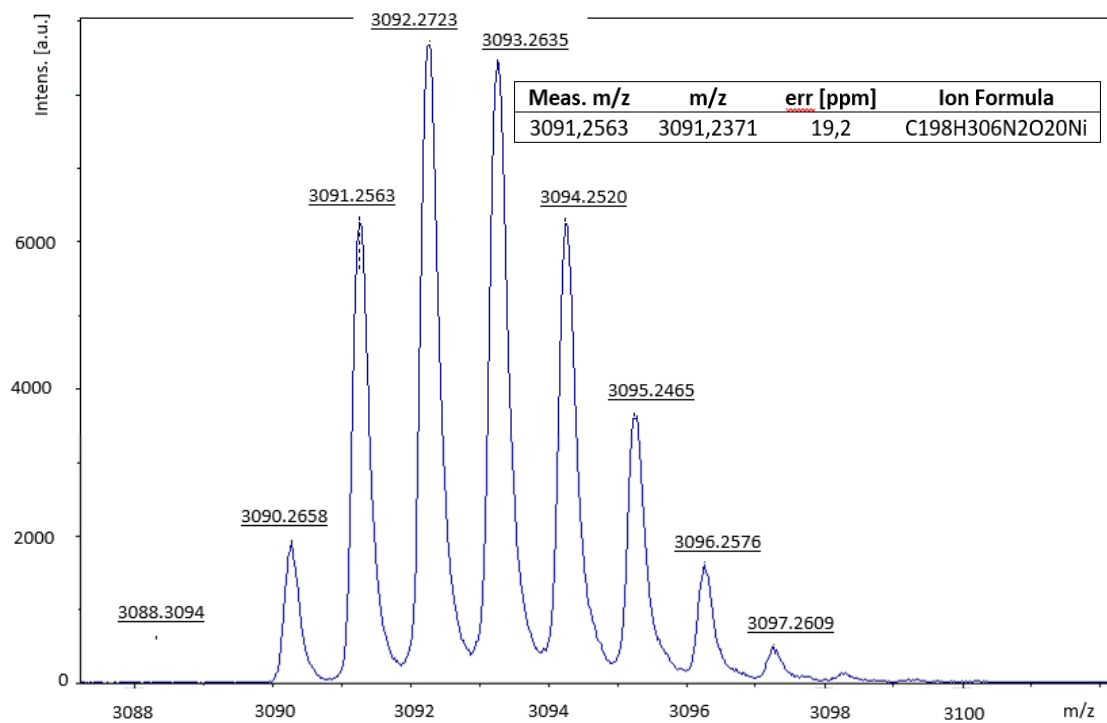


Figure S20: MALDI-TOF mass spectrum of the complex **2a**.

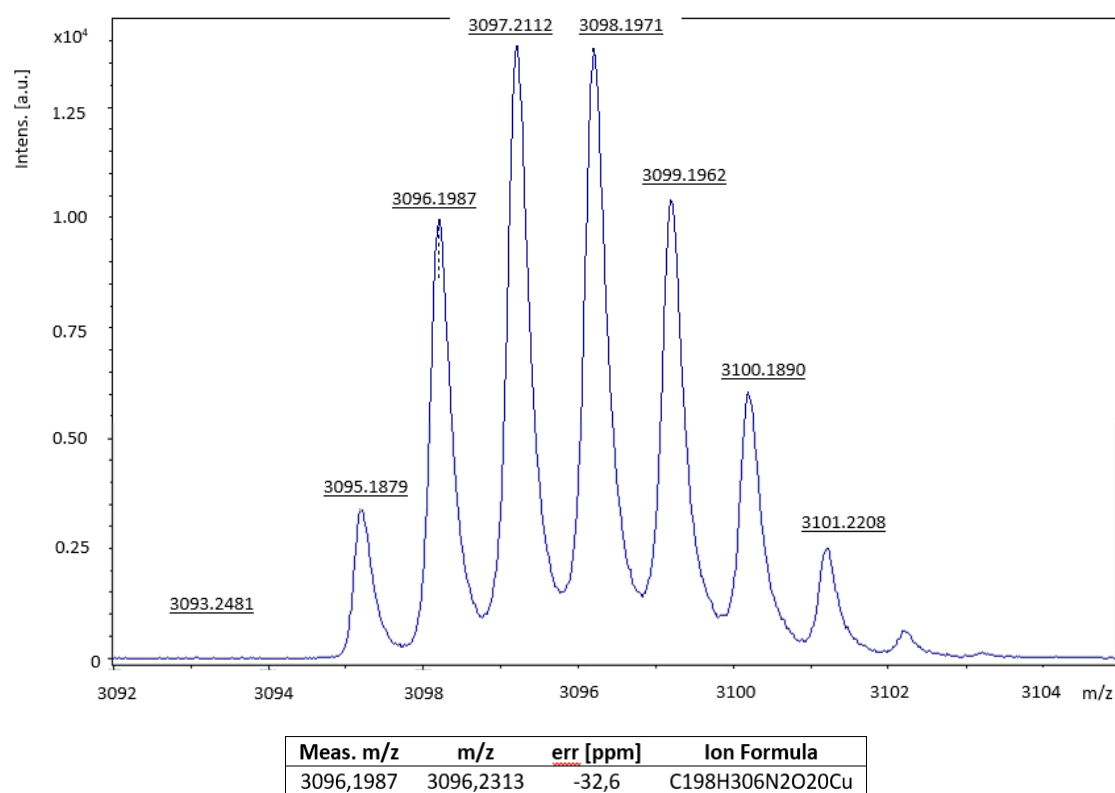


Figure S21: MALDI-TOF mass spectrum of the complex **3a**.

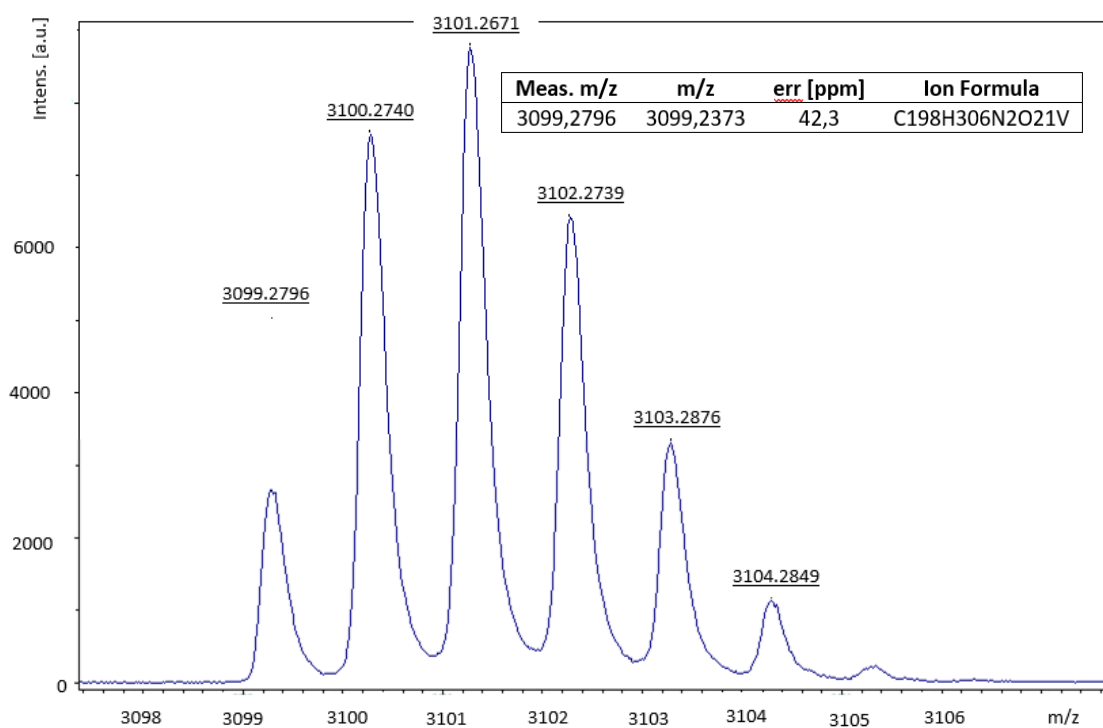


Figure S22: MALDI-TOF mass spectrum of the complex **4a**.

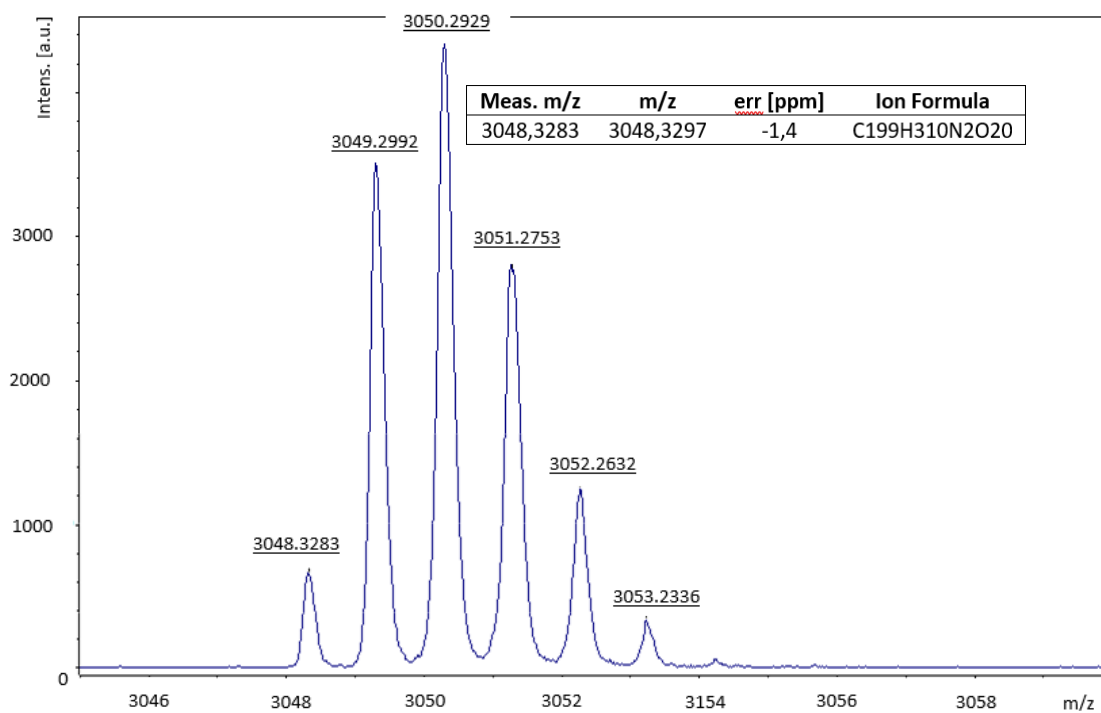


Figure S23: MALDI-TOF mass spectrum of the free ligand Salpn (**1b**).

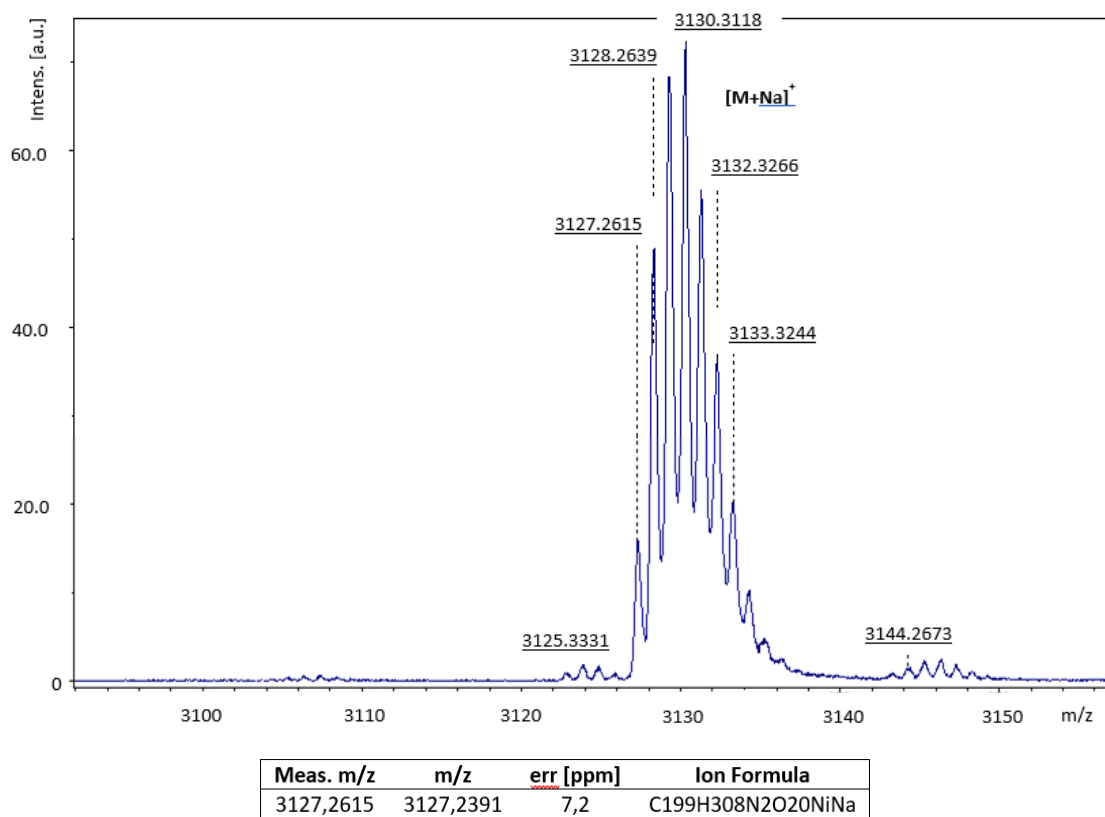


Figure S24: MALDI-TOF mass spectrum of the complex **2b**.

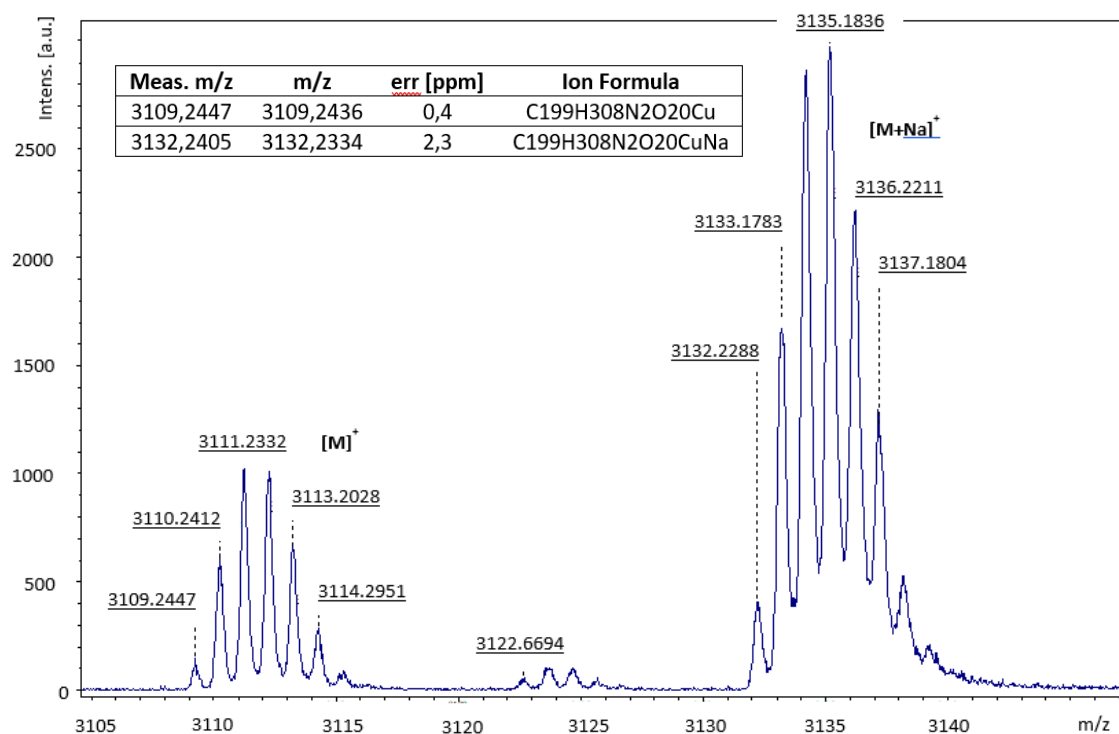


Figure S25: MALDI-TOF mass spectrum of the complex **3b**.

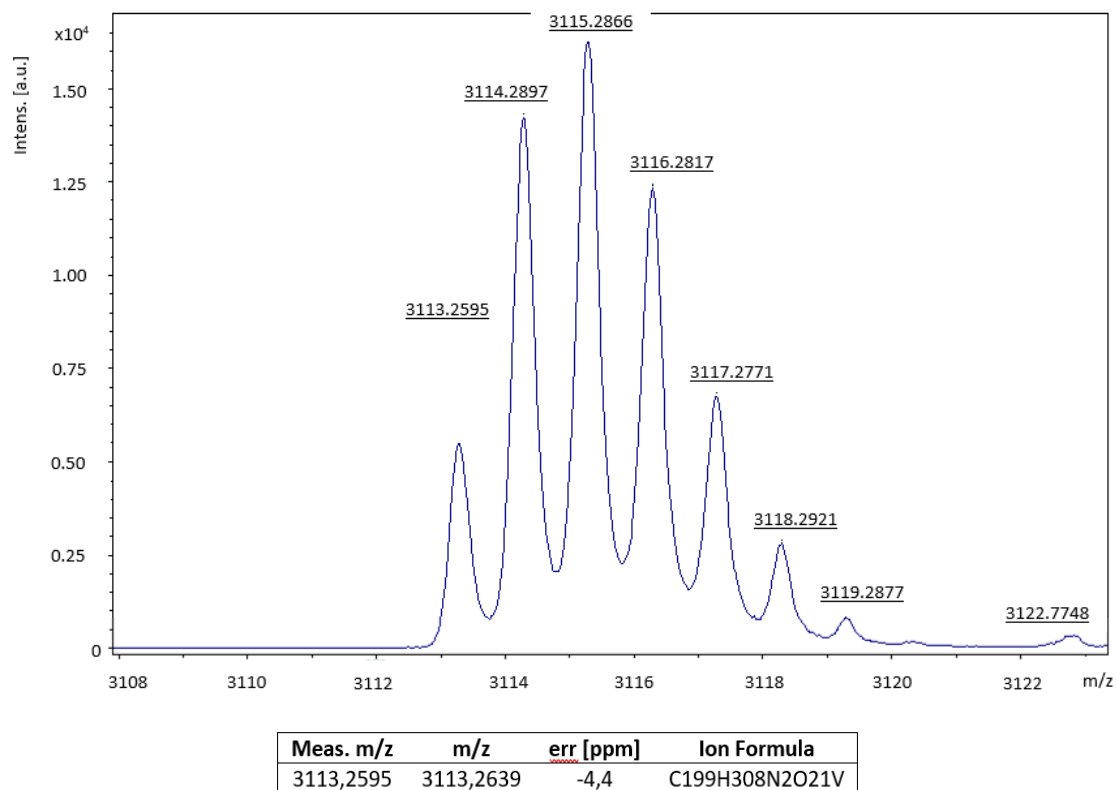


Figure S26: MALDI-TOF mass spectrum of the complex **4b**.

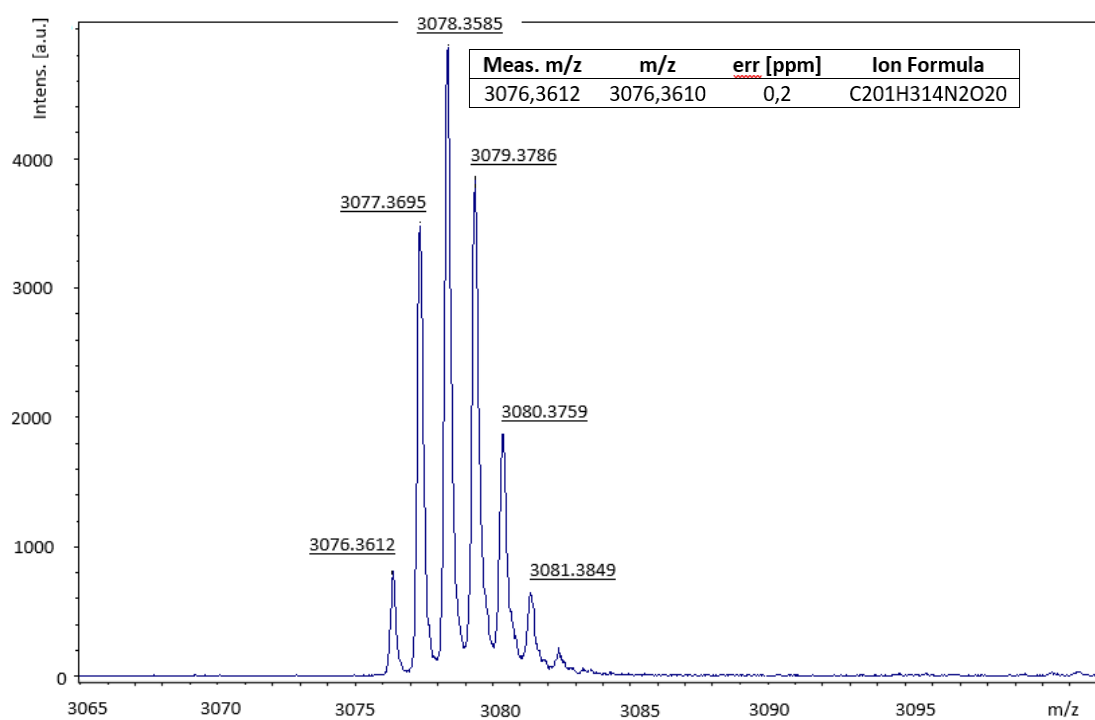


Figure S27: MALDI-TOF mass spectrum of the free ligand Me₂Salpn (**1c**).

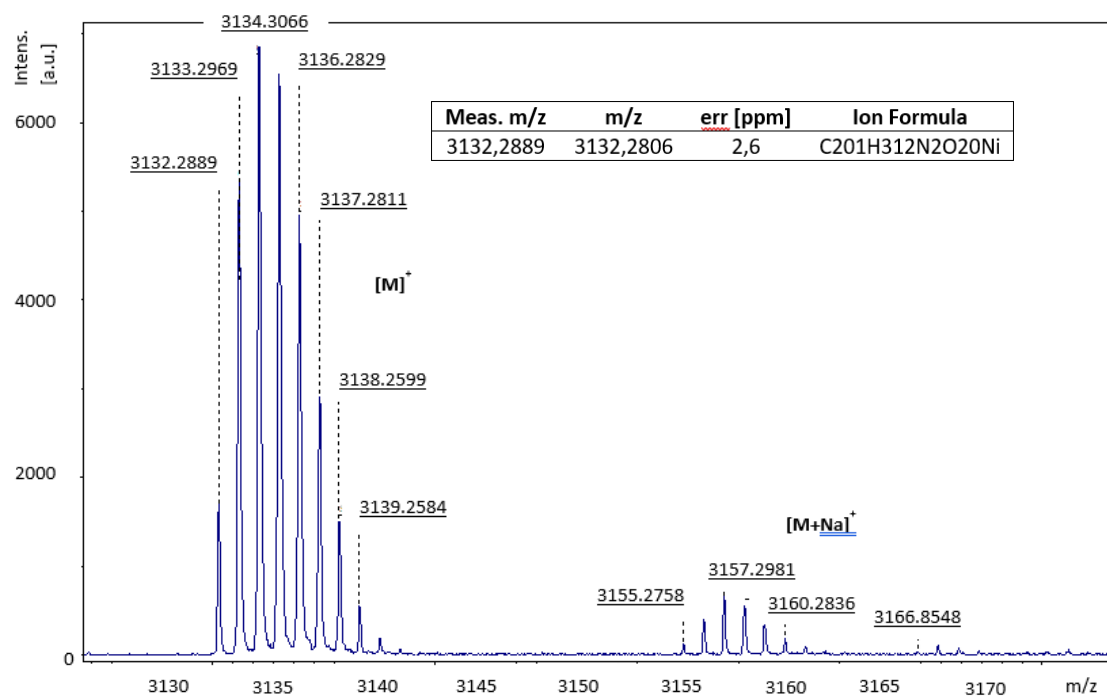


Figure S28: MALDI-TOF mass spectrum of the complex **2c**.

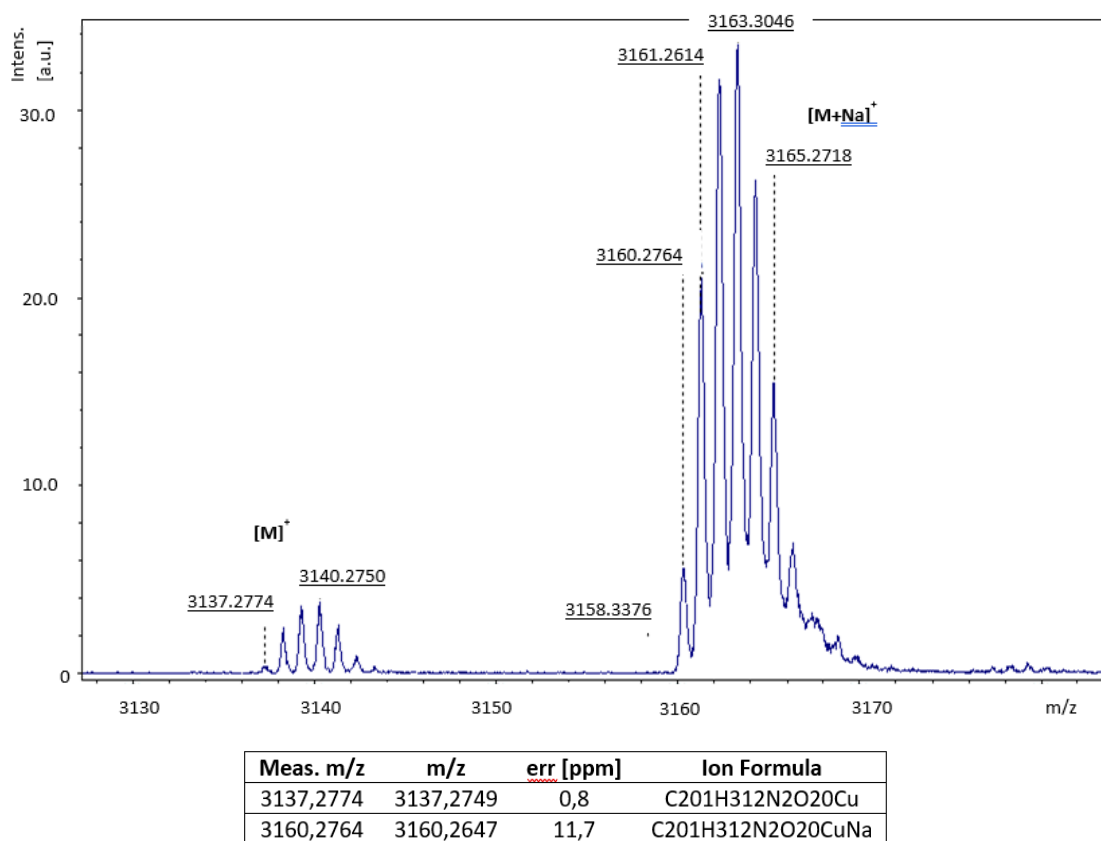


Figure S29: MALDI-TOF mass spectrum of the complex **3c**.

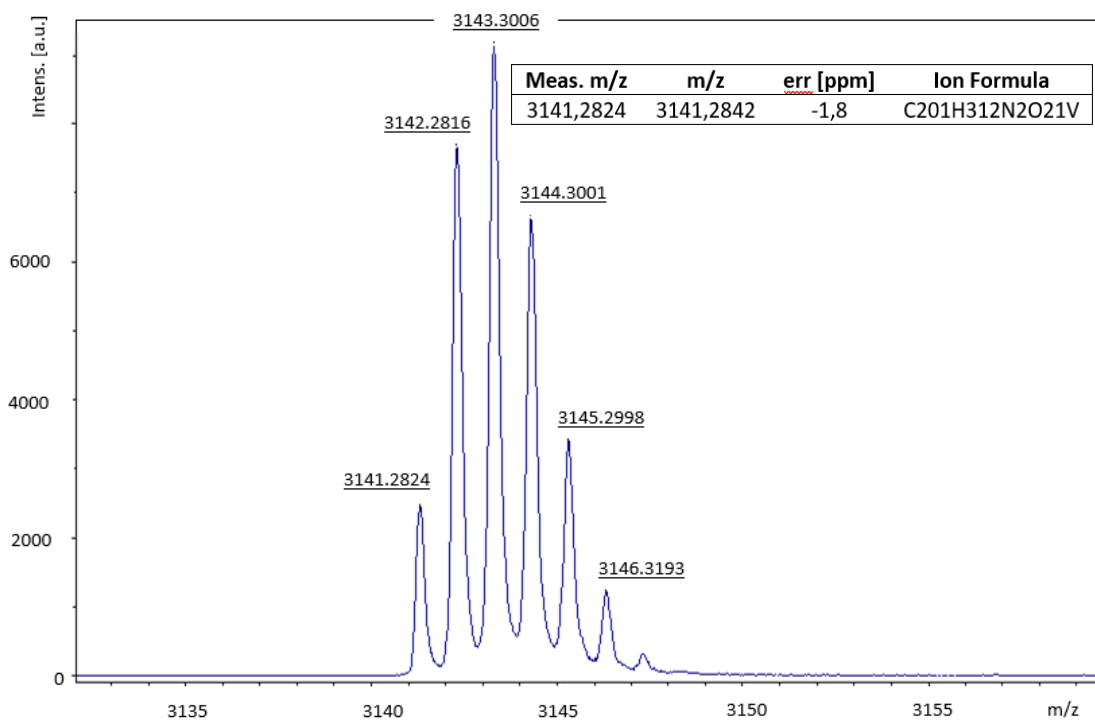


Figure S30: MALDI-TOF mass spectrum of the complex **4c**.

DSC scans: from top to bottom: first heating, first cooling and second heating.

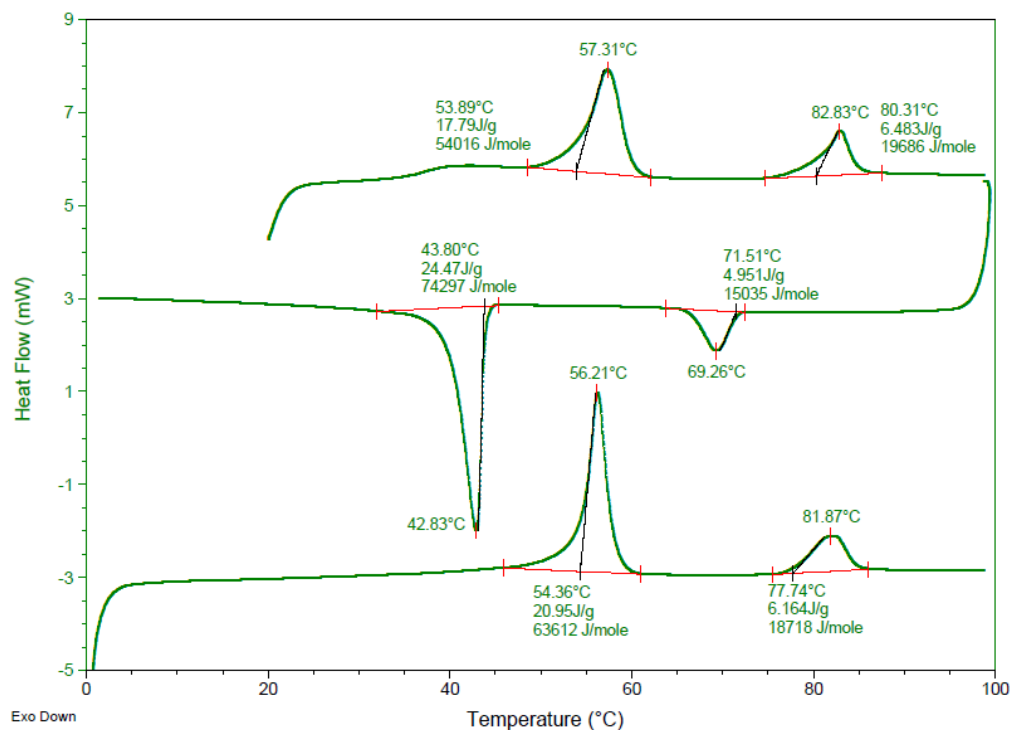


Figure S31: DSC scans of the free ligand Salen (**1a**).

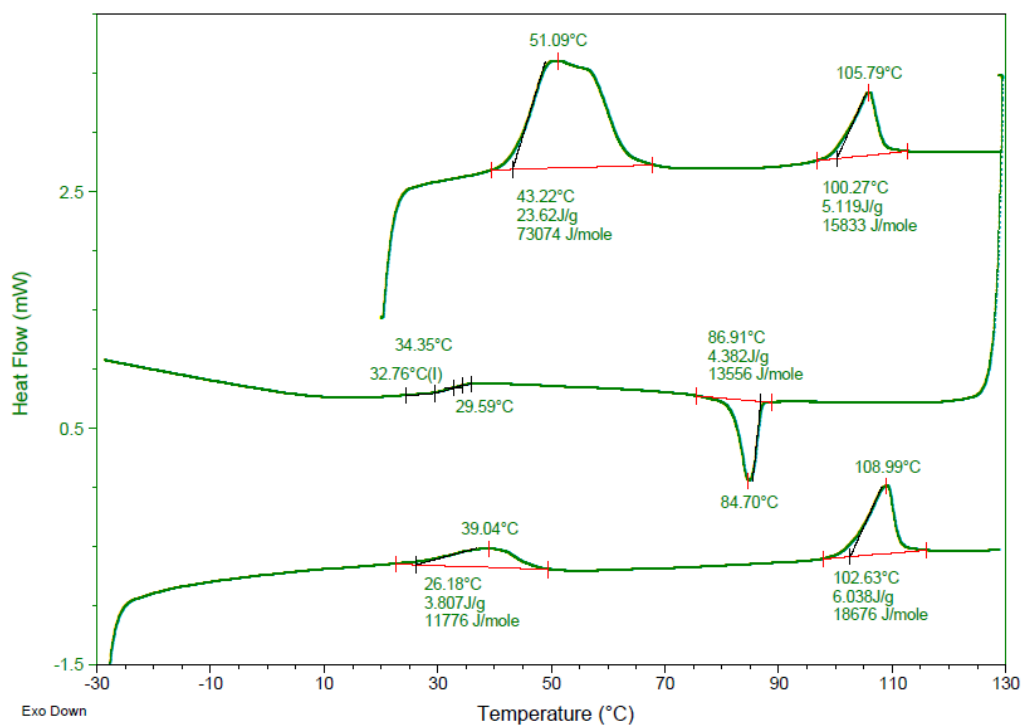


Figure S32: DSC scans of the complex **2a**.

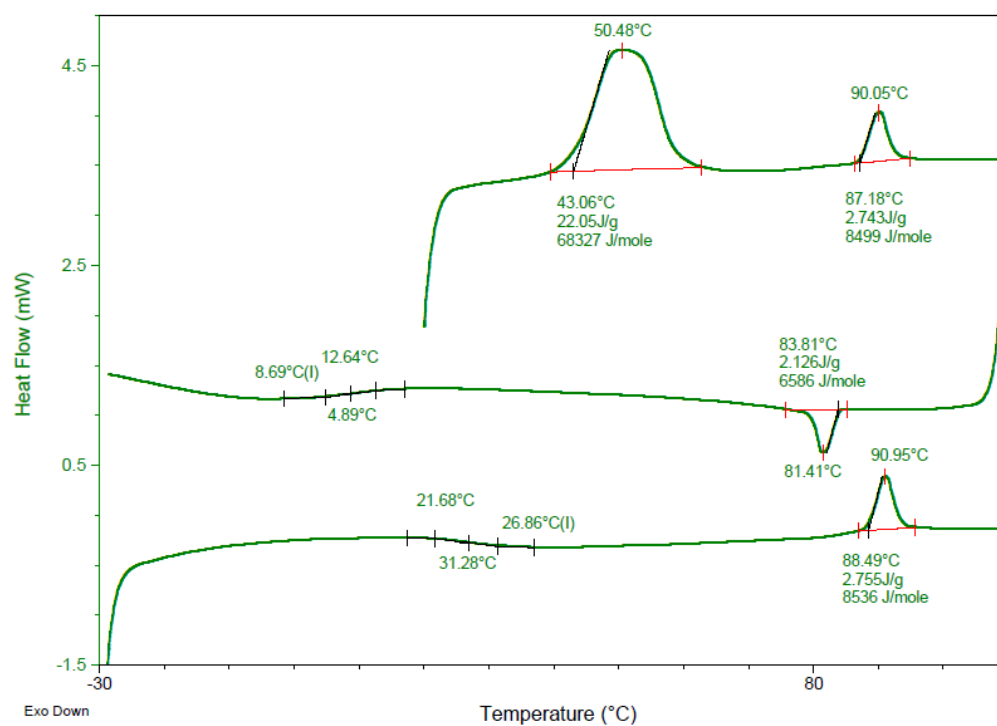


Figure S33: DSC scans of the complex **3a**.

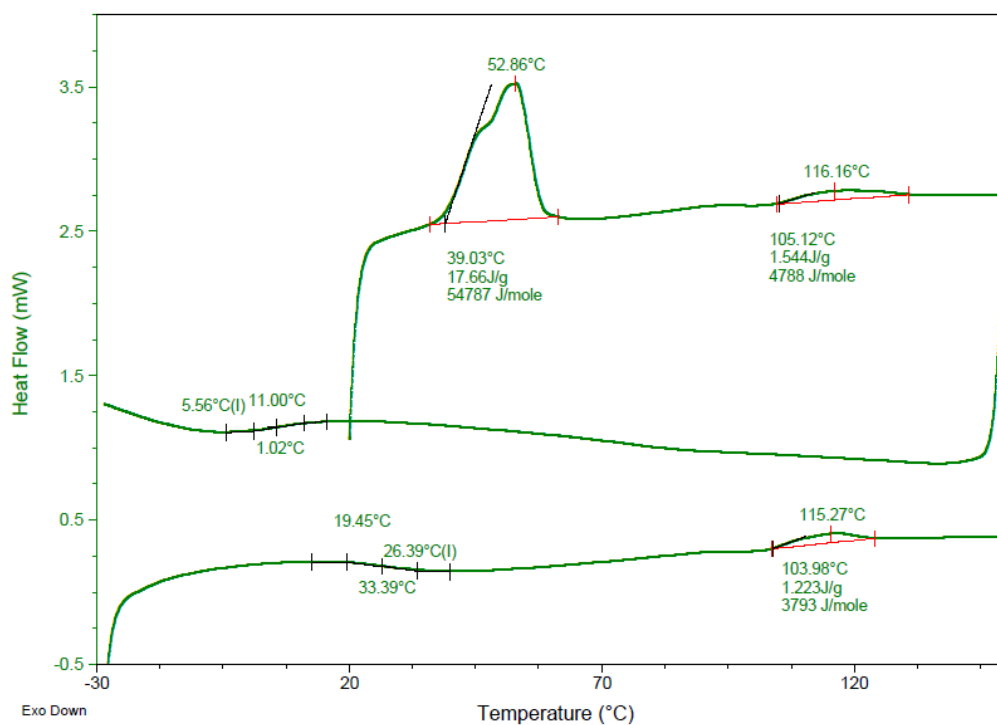


Figure S34: DSC scans of the complex **4a**.

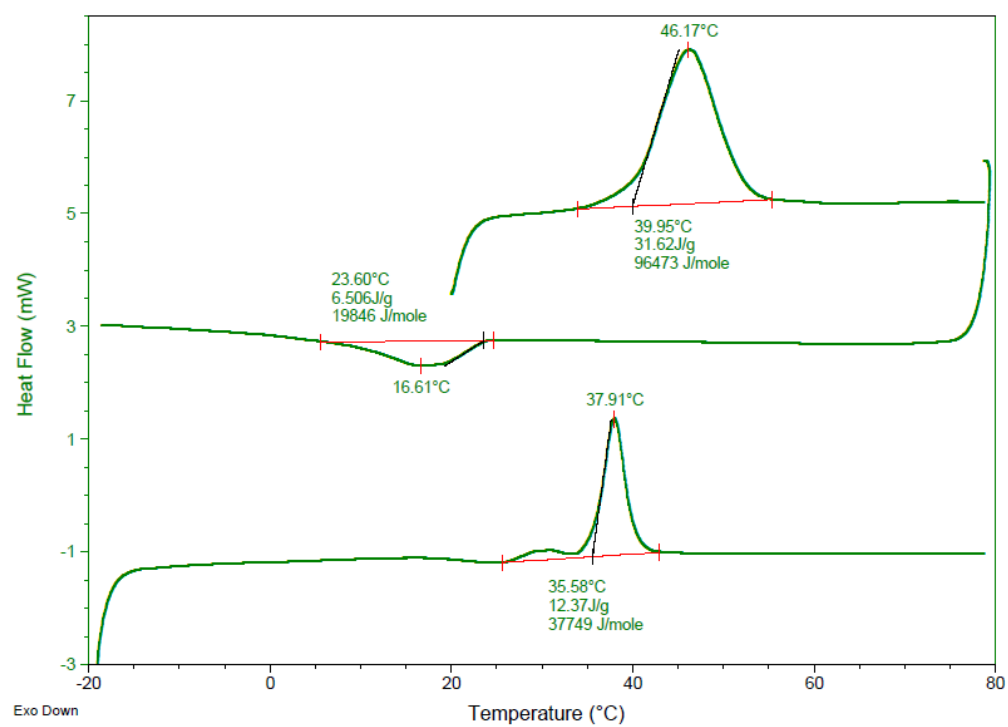


Figure S35: DSC scans of the free ligand Salpn (**1b**).

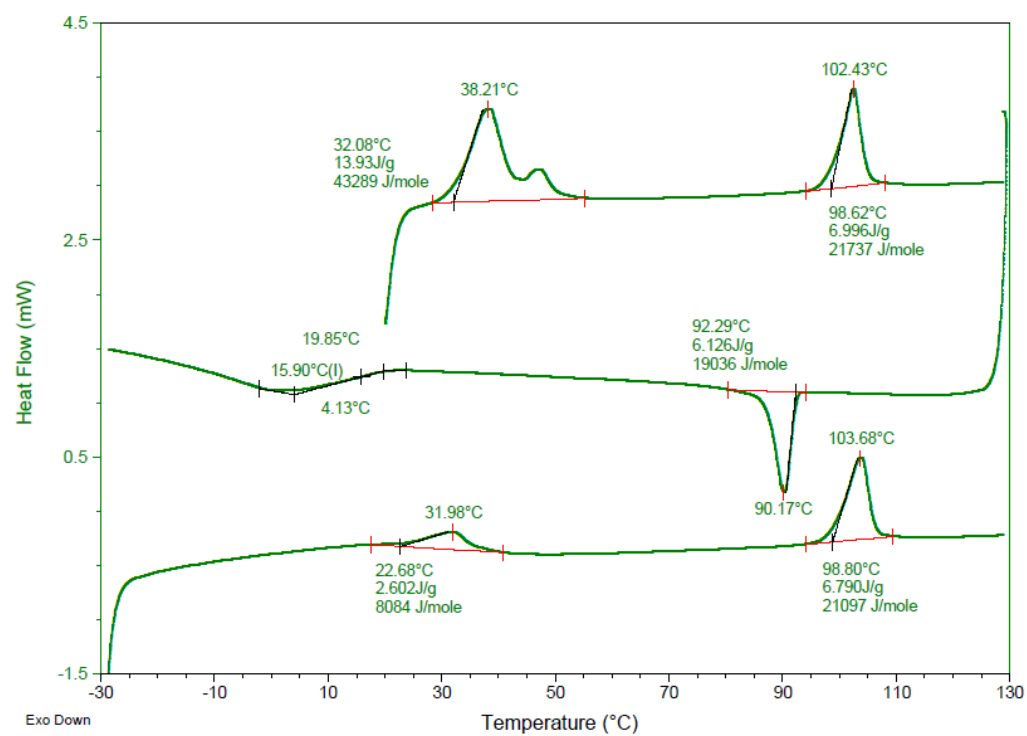


Figure S36: DSC scans of the complex **2b**.

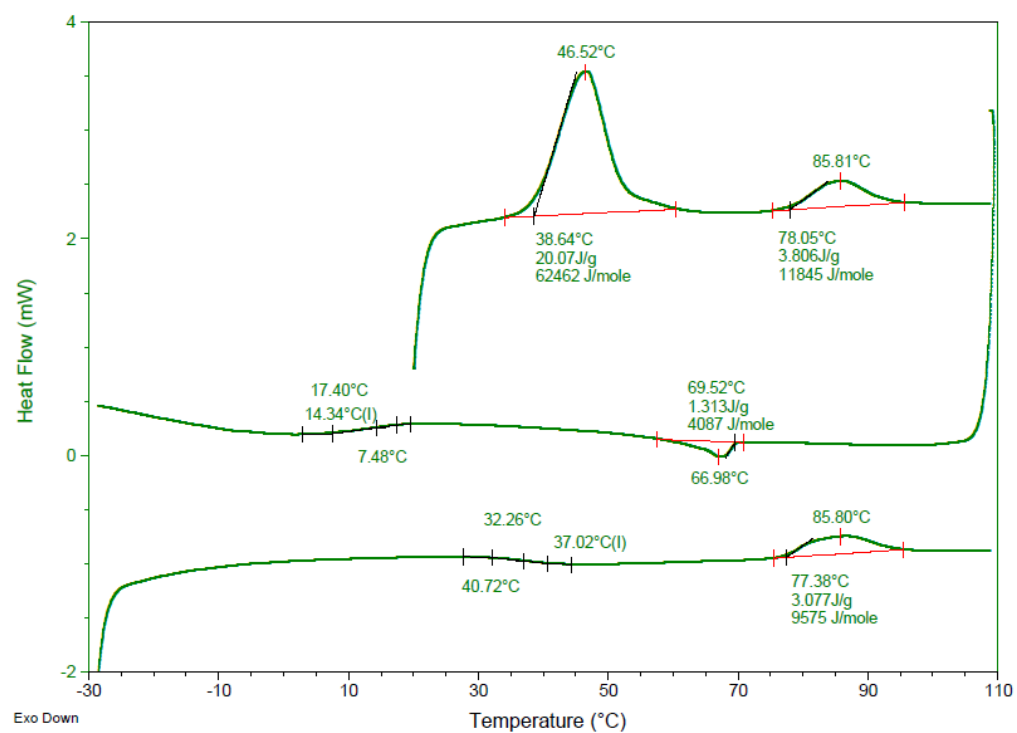


Figure S37: DSC scans of the complex **3b**.

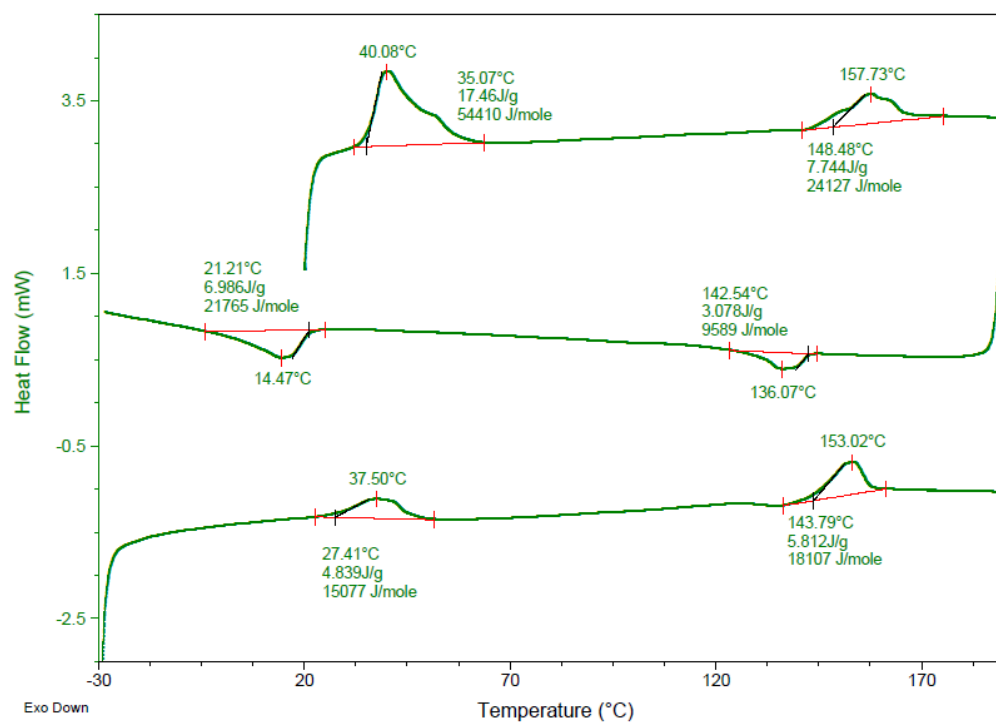


Figure S38: DSC scans of the complex **4b**.

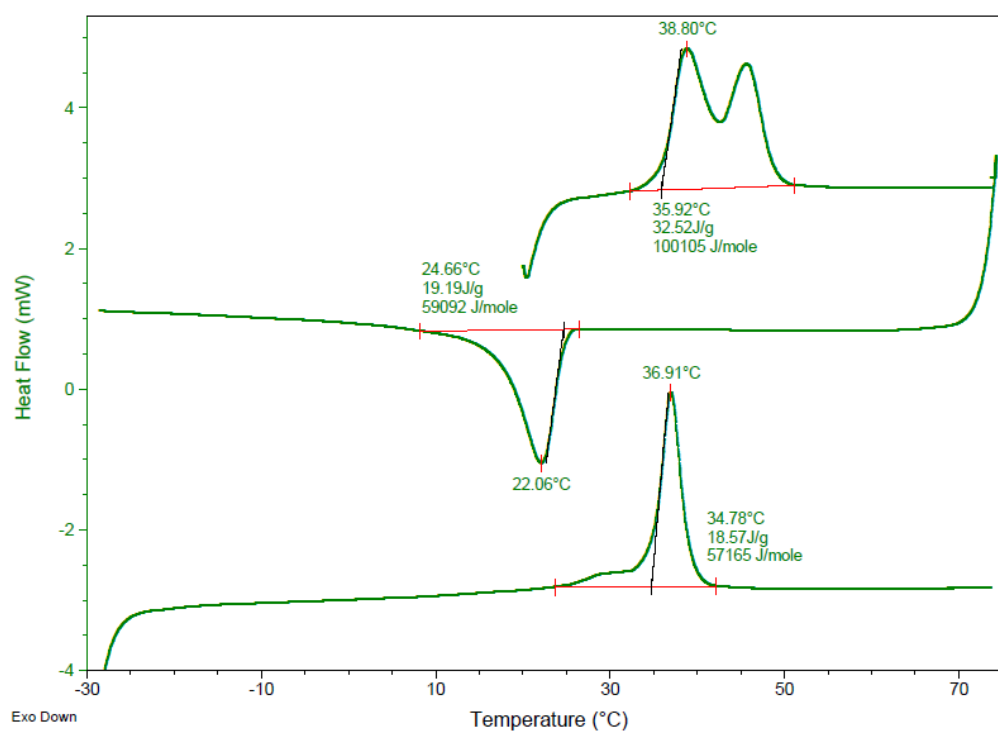


Figure S39: DSC scans of the free ligand Me₂Salpn (**1c**).

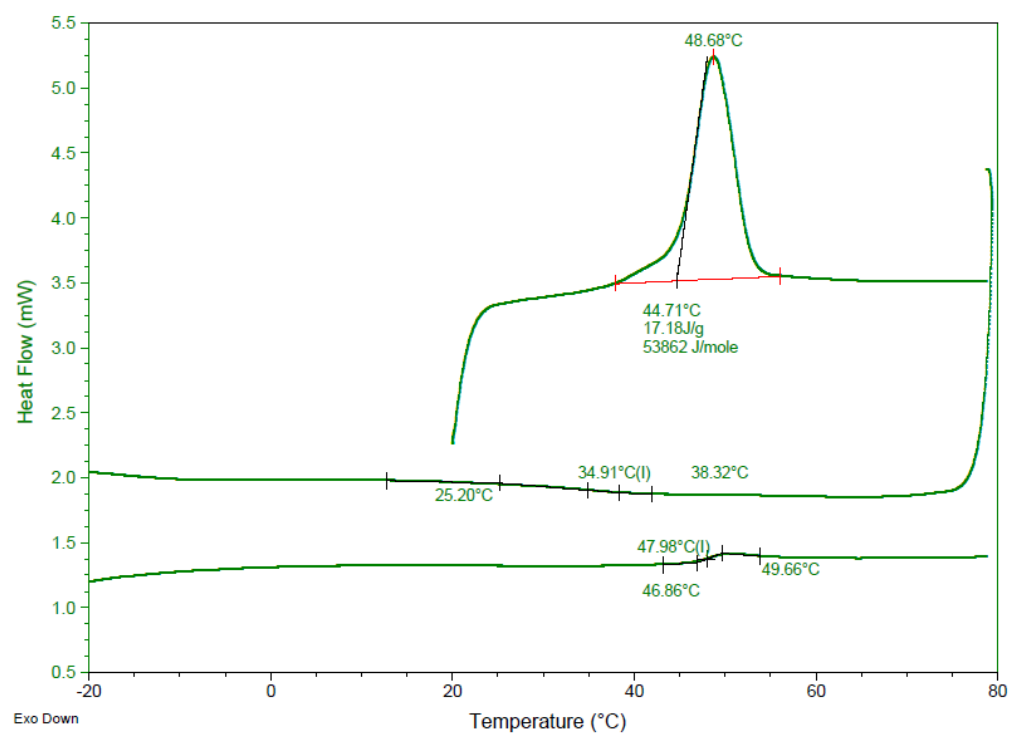


Figure S40: DSC scans of the complex **2c**.

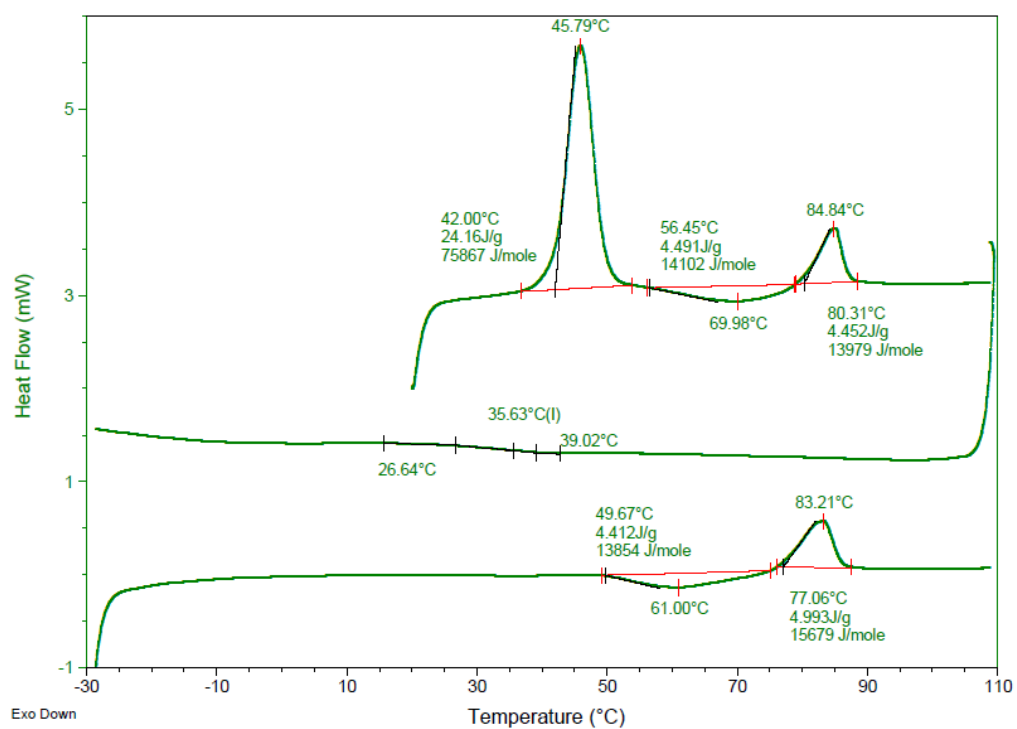


Figure S41: DSC scans of the complex **3c**.

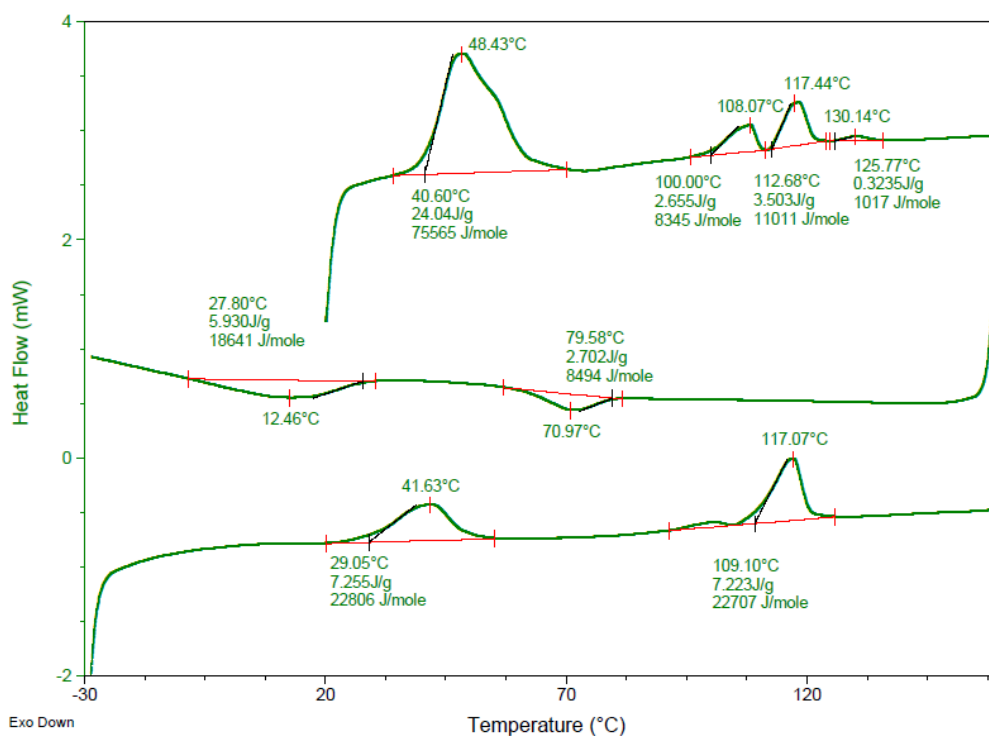


Figure S42: DSC scans of the complex **4c**.

Cyclic voltamograms

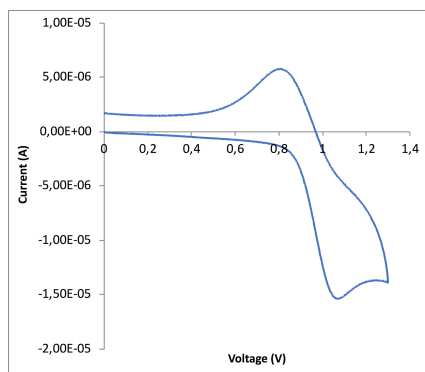


Figure S43. Cyclic voltammogram of **1a**

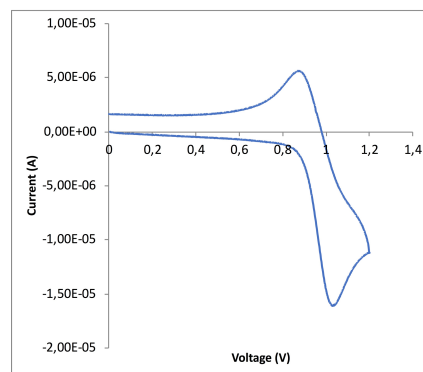


Figure S44. Cyclic voltammogram of **2a**

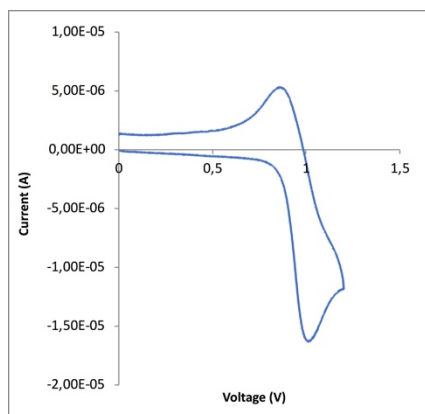


Figure S45. Cyclic voltammogram of **3a**

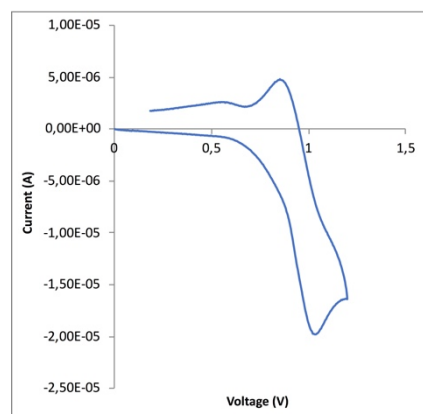


Figure S46. Cyclic voltammogram of **4b**

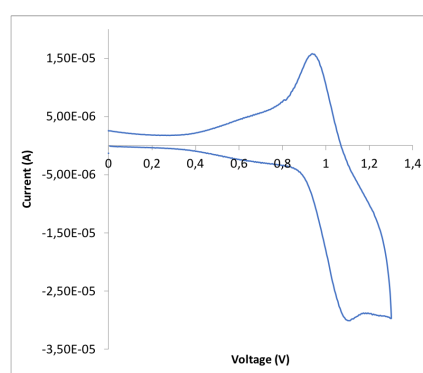
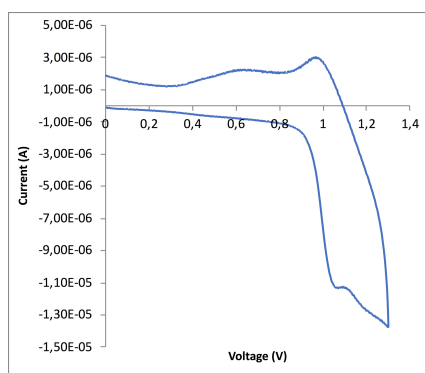


Figure S47. Cyclic voltammograms of [Ni(salen)] (left) and [Ni(salen)] + Triph (right)

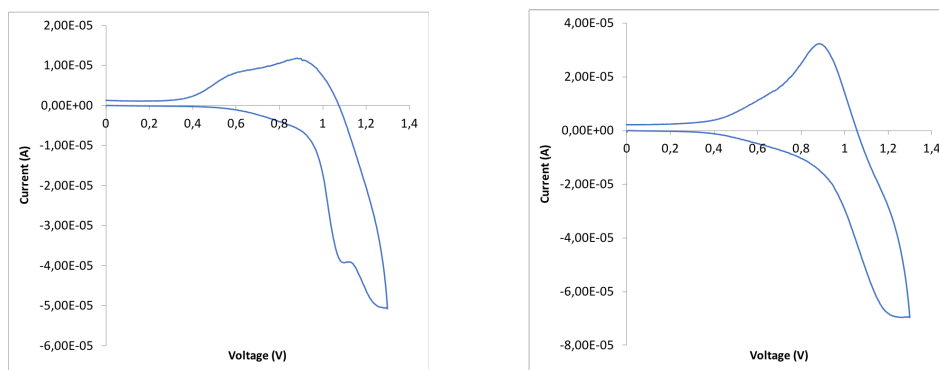


Figure S48. Cyclic voltamograms of [Cu(salen)] (left) and [Cu(salen)] + Triph (right)

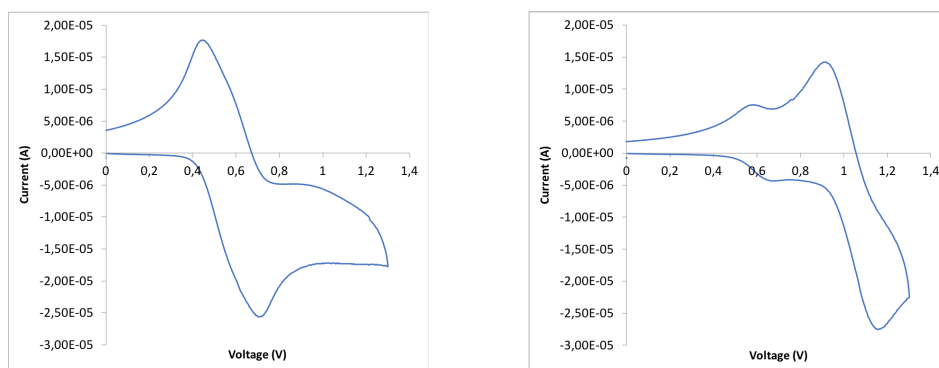


Figure S49. Cyclic voltamograms of [VO(salen)] (left) and [VO(salen)] + Triph (right)

SCLC Measurements

The Space-Charge-Limited Current (SCLC) is a method that can be used to measure the charge mobility in semiconductors. It is performed acquiring the current-voltage characteristics of thin films placed between two suitably chosen electrodes. For semiconductors, a linear increase of the current is observed at low applied voltage, while at higher applied voltages the current can start to be limited from the space-charge field and increases quadratically, following the Mott-Gurney law, in which the effect of the traps is not considered:

$$i = \frac{9}{8} \varepsilon \mu \frac{A V^2}{d^3} \quad (1)$$

where i is the current, μ is the charge mobility, ε is the permittivity of the material, V is the applied voltage and d and A are the thickness and the area of the device, respectively. As an

example, the I/V curve acquired for complex **4b** is shown in Figure S50.

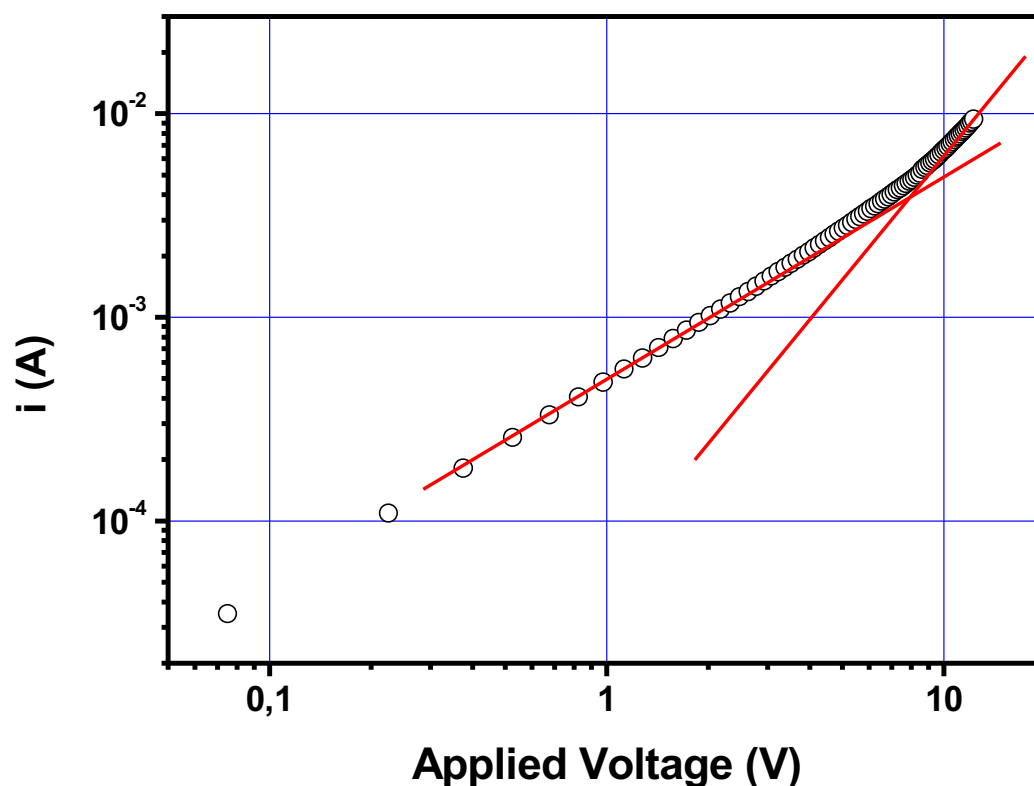


Figure S50: Current vs applied voltage for a sample of complex **4b**. The red lines are not fittings, but show ideal linear and quadratic behavior.

In order to extract meaningful mobility values from such kind of data by using Eqn. 1, the electrodes must work as a charge-reservoir. In other words, the contact between the electrode and the material must be ohmic. This is usually obtained if the difference between the work function of the injecting electrode and the HOMO energy of the material in the case of p-conductors (LUMO level in the case of n-conductors) is not higher than 0.3-0.4 eV. In the case of our materials, it is possible to use gold electrodes since its work function is 5.0-5.1 eV and it matches well the HOMO levels of the compounds.

The samples for Space-Charge Limited Current measurements were fabricated by overlapping one glass substrate covered with three gold stripes with another one covered by five ITO stripes,

controlling the thickness by glass spacers. In this way, it is possible to obtain samples with 15 independent overlapping areas. The samples thickness was determined by interferometry and varied between 7 and 12 μm . Commercial glasses fully covered by ITO (Visiontek $12\Omega/\text{sq.}$, 120 nm thick ITO) were used to obtain, by photolithography, the five stripes, while the gold electrodes were deposited on bare glass by evaporation under vacuum. To prepare the samples, the empty cells were placed on a hot plate, with some of the compound on one side, heating up to 20°C above the melting point, to allow the cell filling by capillarity. After the material completely filled the cell, the temperature was decreased. In order to induce a more homogeneous homeotropic alignment of the mesophase, a thermal annealing procedure was carried out: the sample was reheated up to the isotropic phase and then it was cooled at $0.1^\circ\text{C}/\text{min}$ down to 0.5°C below the clearing point, maintaining that temperature for 600 minutes. At this point, the sample was cooled down to room temperature at a rate of $0.1^\circ\text{C}/\text{min}$. In the present case, such a process was ineffective. In fact, samples of all complexes already showed either homogeneous homeotropic alignment (complex **2a**) or quasi-homeotropic alignment (complexes **3a** and **4b**) without any thermal annealing and the annealing did not change the alignment. In contrast, the alignment of ligand **1a** was never homogeneous, even after repeated thermal annealing cycles.

An electrometer, either a Keithley 6517A or a Keithley 2636B, was used to acquire current / voltage characteristics, while the dielectric constant was obtained from capacity measurements performed on a HP 4284A Precision LCR Meter.

Low-angle X-ray diffraction diagrams.

Figure S51 collects, for the low-angle X-ray diagrams of the materials in Table 2, the patterns not shown in the main text.

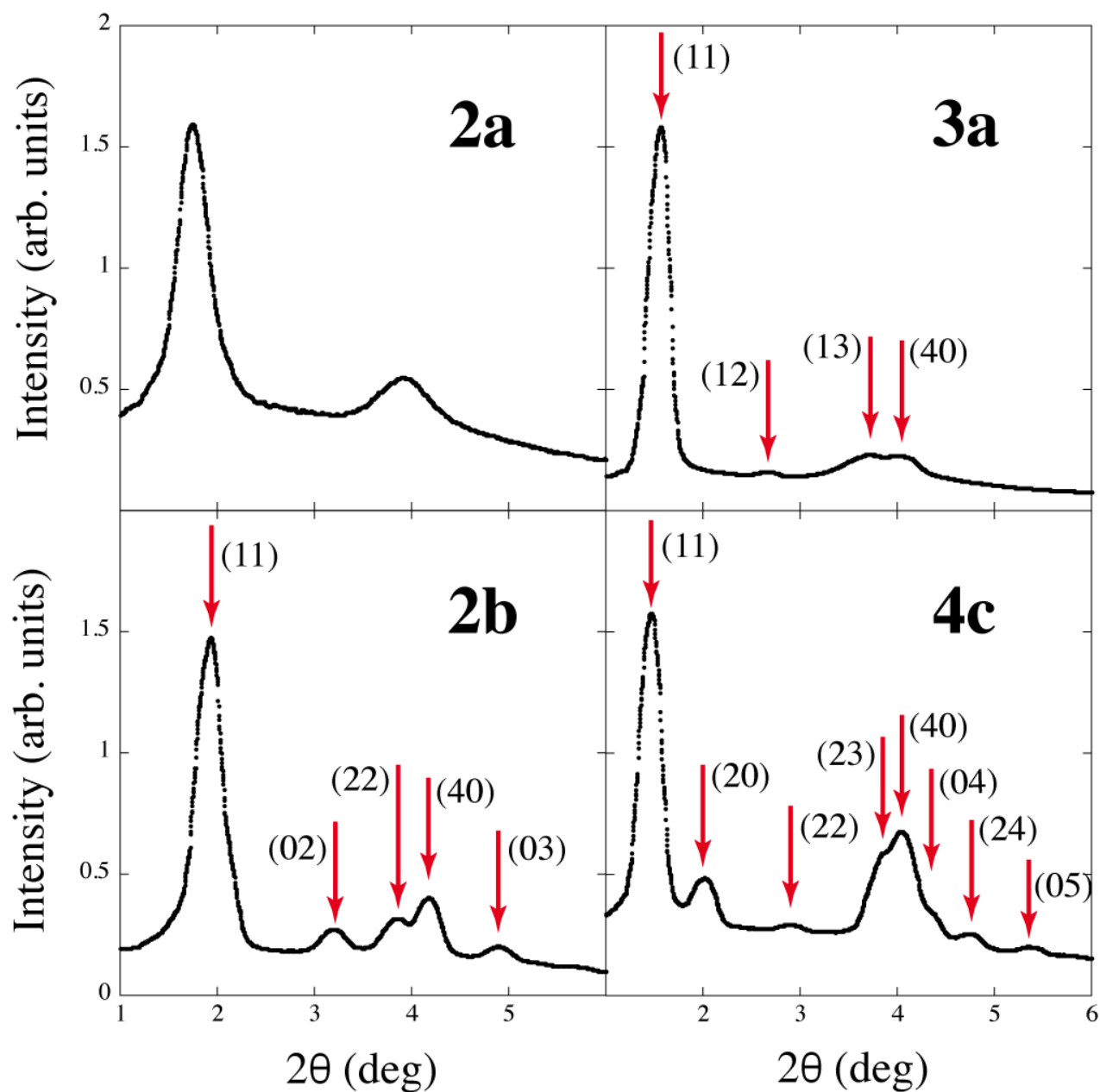


Figure S51. Low-angle X-ray patterns of compounds **2a**, **3a**, **2b**, and **4c**. The arrows indicate the positions of the (hk) reflections corresponding to the columnar 2D lattice. Compound **2a** is a columnar nematic.

The low-angle X-ray diagram of the free ligand is shown in Figure S52.

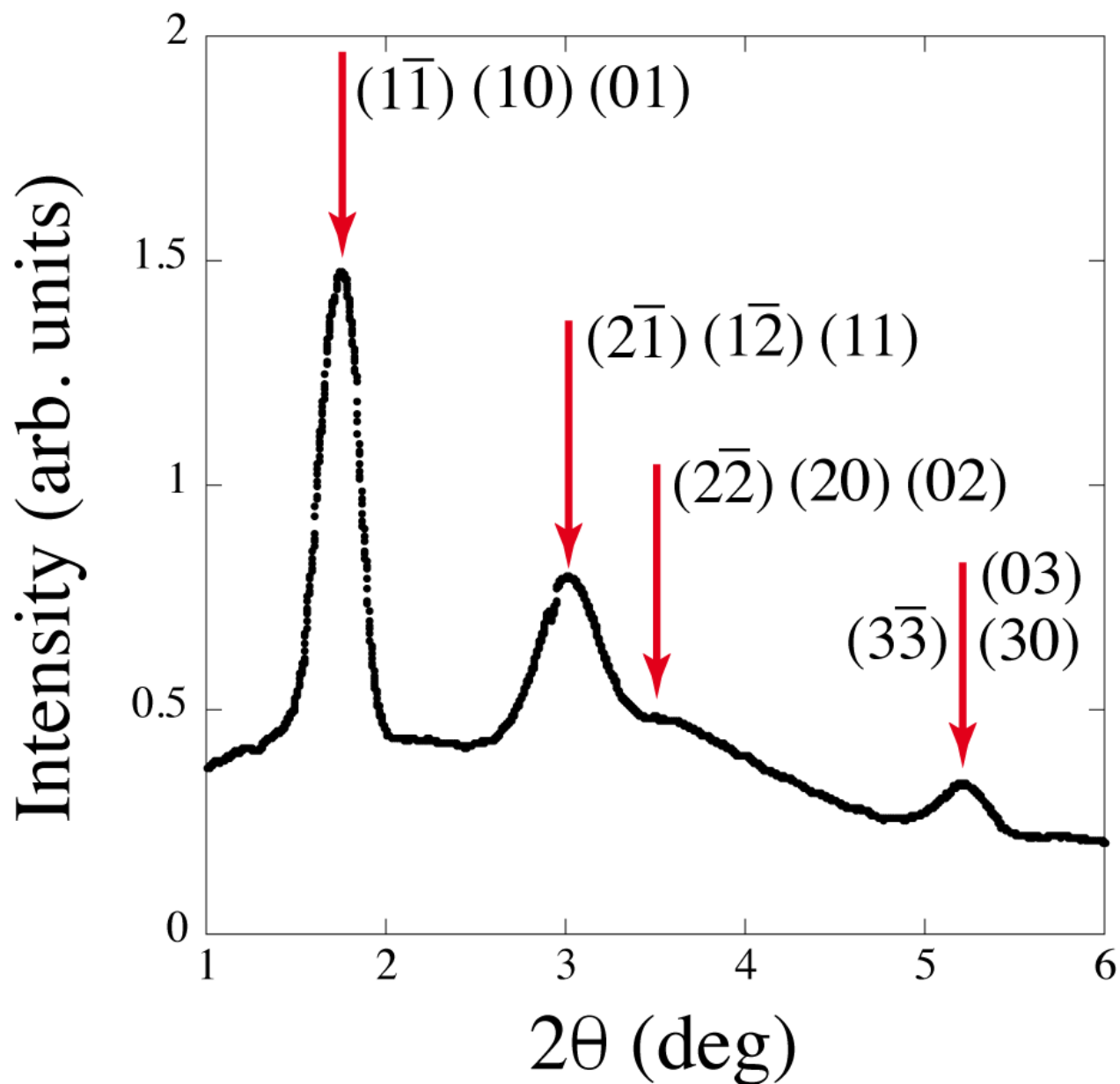


Figure S52. Low-angle X-ray pattern of compound **1a**. The arrows indicate the positions of the (hk) reflections corresponding to the 2D lattice of the hexagonal columnar structure.

References

- ¹ Feringán, B.; Romero, P.; Serrano, J. L.; Folcia, C. L.; Etxebarria, J.; Ortega, J.; Termine, R.; Golemme, A.; Giménez, R.; Sierra, T. H Bonded Donor–Acceptor Units Segregated in Coaxial Columnar Assemblies: Toward High Mobility Ambipolar Organic Semiconductors. Segregated Donor–Acceptor Columns in Liquid Crystals That Exhibit Highly Efficient Ambipolar Charge Transport. *J. Am. Chem. Soc.* **2016**, *138*, 12511–12518.
- ² Tritto, E.; Chico, R.; Sanz-Enguita, G.; Folcia, C. L.; Ortega, J.; Coco, S.; Espinet, P. Alignment of Palladium Complexes into Columnar Liquid Crystals Driven by Peripheral Triphenylene Substituents. *Inorg. Chem.* **2014**, *53*, 3449–3455.
- ³ Bushby, R. J.; Boden, N.; Kilner, C. A.; Lozman, O. R.; Lu, Z.; Liu, Q.; Thornton-Pett M. A. Helical geometry and liquid crystalline properties of 2,3,6,7,10,11-hexaalkoxy-1-nitrotriphenylenes. *J. Mater. Chem.* **2003**, *13*, 470–474.
- ⁴ Zolezzi, S.; Decinti, A.; Spodine, E. Syntheses and characterization of copper(II) complexes with Schiff-base ligands derived from ethylenediamine, diphenylethylenediamine and nitro, bromo and methoxy salicylaldehyde. *Polyhedron* **1999**, *18*, 897–904.
- ⁵ Vafazadeh, R.; Bagheri, M. Kinetics and Mechanism of the Ligand Exchange Reaction Between Tetradentate Schiff Base N,N'-ethylen-bis (salicylaldimine) and Ni(N,N'-propylen-bis(salicylaldimine)). *S. Afr. J. Chem.* **2015**, *68*, 21–26.
- ⁶ Białek, M.; Leksza, A.; Piechota, A.; Kurzak, K.; Koprek, K. Oxovanadium(IV) complexes with [ONNO]-chelating ligands as catalysts for ethylene homo- and copolymerization. *J. Polym. Res.* **2014**, *21*, 389–400.